



Mechanisms of PTP σ -Mediated Presynaptic Differentiation

Claire Bomkamp¹, Nirmala Padmanabhan^{2,3,4}, Benyamin Karimi^{2,3,4}, Yuan Ge¹, Jesse T. Chao⁵, Christopher J. R. Loewen⁵, Tabrez J. Siddiqui^{2,3,4} and Ann Marie Craig^{1*}

¹Djavad Mowafaghian Centre for Brain Health, Department of Psychiatry, University of British Columbia, Vancouver, BC, Canada, ²Health Sciences Centre, Kleysen Institute for Advanced Medicine, University of Manitoba, Winnipeg, MB, Canada, ³Department of Physiology and Pathophysiology, Rady Faculty of Health Sciences, University of Manitoba, Winnipeg, MB, Canada, ⁴The Children's Hospital Research Institute of Manitoba (CHRIM), Winnipeg, MB, Canada, ⁵Department of Cellular and Physiological Sciences, Faculty of Medicine, Life Sciences Institute, University of British Columbia, Vancouver, BC, Canada

Formation of synapses between neurons depends in part on binding between axonal and dendritic cell surface synaptic organizing proteins, which recruit components of the developing presynaptic and postsynaptic specializations. One of these presynaptic organizing molecules is protein tyrosine phosphatase σ (PTP σ). Although the protein domains involved in adhesion between PTP σ and its postsynaptic binding partners are known, the mechanisms by which it signals into the presynaptic neuron to recruit synaptic vesicles and other necessary components for regulated transmitter release are not well understood. One attractive candidate to mediate this function is liprin- α , a scaffolding protein with well-established roles at the synapse. We systematically mutated residues of the PTP σ intracellular region (ICR) and used the yeast dihydrofolate reductase (DHFR) protein complementation assay to screen for disrupted interactions between these mutant forms of PTP σ and its various binding partners. Using a molecular replacement strategy, we show that disrupting the interaction between PTP σ and liprin- α , but not between PTP σ and itself or another binding partner, caskin, abolishes presynaptic differentiation. Furthermore, phosphatase activity of PTP σ and binding to extracellular heparan sulfate (HS) proteoglycans are dispensable for presynaptic induction. Previous reports have suggested that binding between PTP σ and liprin- α is mediated by the PTP σ membrane-distal phosphatase-like domain. However, we provide evidence here that both of the PTP σ phosphatase-like domains mediate binding to liprin- α and are required for PTP σ -mediated presynaptic differentiation. These findings further our understanding of the mechanistic basis by which PTP σ acts as a presynaptic organizer.

Keywords: synapse, synaptogenesis, LAR-RPTP, phosphatase, adhesion proteins, liprin, scaffolding proteins

OPEN ACCESS

Edited by:

Carlos B. Duarte,
University of Coimbra, Portugal

Reviewed by:

Shuya Fukai,
The University of Tokyo, Japan
Kurt Gottmann,
Heinrich Heine Universität Düsseldorf,
Germany

*Correspondence:

Ann Marie Craig
acraig@mail.ubc.ca

Received: 12 March 2019

Accepted: 06 May 2019

Published: 22 May 2019

Citation:

Bomkamp C, Padmanabhan N, Karimi B, Ge Y, Chao JT, Loewen CJR, Siddiqui TJ and Craig AM (2019) Mechanisms of PTP σ -Mediated Presynaptic Differentiation. *Front. Synaptic Neurosci.* 11:17. doi: 10.3389/fnsyn.2019.00017

INTRODUCTION

A key early step in the formation of a new synapse involves binding between synaptic organizing proteins expressed on the axon of one neuron and the dendrite of another, which triggers clustering of intracellular synaptic proteins in both neurons. The presentation of a single synaptic organizing protein expressed on the surface of a non-neuronal cell is sufficient to induce local clustering of presynaptic or postsynaptic machinery. This is exemplified by the first discovered and best known pair of synaptic organizing proteins, the postsynaptic neuroligins (Scheiffele et al., 2000) and the presynaptic neurexins (Graf et al., 2004). In addition to

the neuroligins and neurexins, a variety of other organizing proteins with similar synaptogenic activities have been described (Südhof, 2018). These include the presynaptically-expressed LAR, protein tyrosine phosphatase σ (PTP σ), and PTP δ , which together make up the LAR-RPTP family and interact with postsynaptic NGL-3 (Woo et al., 2009), TrkC (Takahashi et al., 2011), Slitrk1-6 (Takahashi et al., 2012; Um et al., 2014), IL1RAPL1 (Yoshida et al., 2011), IL1RACp (Yoshida et al., 2012), SALM3, and SALM5 (Mah et al., 2010; Li et al., 2015).

The mechanism by which synaptic organizing proteins signal the formation of a nascent synapse must involve more than simply adhesion. In the case of neurexin, recruitment of intracellular proteins can occur at least under some circumstances without the presence of the neurexin intracellular region (ICR; Gokce and Südhof, 2013), presumably through an unidentified co-receptor. The same does not appear to be true for the LAR-RPTPs, since a version of PTP σ lacking its ICR acted as a dominant-negative suppressor of synaptogenesis (Takahashi et al., 2011). However, the mechanism by which these proteins exert their effects, including which intracellular interacting proteins and/or co-receptors are involved, is poorly understood.

LAR-RPTPs are comprised of extracellular Ig and FNIII domains which mediate binding to postsynaptic NGL-3, TrkC, Slitrks, IL1RAPL1, IL1RACp, and SALM ligands (Takahashi and Craig, 2013). The LAR-RPTP Ig1 domain also binds chondroitin sulfate and heparan sulfate (HS), interactions that regulate axon growth (Aricescu et al., 2002; Shen et al., 2009). In the context of synaptogenesis, HS competes with TrkC for PTP σ binding (Coles et al., 2014) but HS may mediate the formation of additional synaptogenic complexes as suggested for a PTP σ -glypican-4-LRRTM4 complex (Ko et al., 2015). The other major family of presynaptic organizers, neurexins, are HSPGs (Zhang et al., 2018). It is not yet clear whether HS-mediated LAR-RPTP interaction with neurexins or other axonal co-receptors may contribute to synaptogenic function.

Following the single transmembrane domain, the LAR-RPTPs have a small wedge domain followed by two phosphatase-like domains, termed D1 and D2, of which only D1 is catalytically active (Streuli et al., 1990; Takahashi and Craig, 2013). There are several known enzymatic substrates of the LAR-RPTPs including p250GAP (Chagnon et al., 2010), β -catenin (Müller et al., 1999; Dunah et al., 2005), and N-cadherin (Siu et al., 2007), which could potentially mediate their synaptogenic effects. The D2 domain binds to the scaffolding proteins of the liprin- α family (Serra-Pagès et al., 1995), the GEF/kinase trio (Debant et al., 1996), and to the CASK-interacting proteins caskin1 and caskin2 (Weng et al., 2011).

Whereas there is little evidence for roles of trio (Astigarraga et al., 2010) or caskin (Weng et al., 2011) in synapse development, considerable genetic and functional evidence from multiple systems implicate liprin- α in presynaptic differentiation. The liprin- α sterile alpha motif (SAM) domains bind CASK (Olsen et al., 2005; Wei et al., 2011), liprin- β (Serra-Pagès et al., 1998), mSyd-1a (Wentzel et al., 2013), and PTP σ (Serra-Pagès et al., 1995). The liprin- α coiled coil domains bind RIM (Schoch et al., 2002) and ELKS (Ko et al., 2003) as

well as liprin- α itself (Serra-Pagès et al., 1998). Thus, liprin- α may function as a “hub” for recruitment of other presynaptic molecules. The *C. elegans* homolog of liprin- α is required for normal synapse morphogenesis and synaptic transmission, and its loss results in the mislocalization of multiple presynaptic components (Zhen and Jin, 1999). Additionally, the homologs of the LAR-RPTPs and liprin- α interact genetically in the context of synapse formation in both *C. elegans* (Ackley et al., 2005) and *Drosophila* (Kaufmann et al., 2002). The role of the mammalian liprin- α family, which contains four members (termed liprin- α 1–liprin- α 4) encoded by four separate genes, is less well characterized. Liprin- α 2 and liprin- α 3 are the most abundant liprin- α isoforms in the brain (Zürner and Schoch, 2009), show different but overlapping expression patterns, and colocalize with synaptic markers (Spangler et al., 2011; Zürner et al., 2011). Knockdown of liprin- α 2 leads to defects in presynaptic release as well as reduced localization of several presynaptic components including CASK and RIM (Spangler et al., 2013). Hippocampal neurons from mice with a knockout of liprin- α 3 show defects in synaptic vesicle docking, tethering, and exocytosis (Wong et al., 2018). Together, these observations point to liprin- α as an attractive candidate for mediating presynaptic differentiation in response to binding between LAR-RPTPs and their postsynaptic partners.

Here, we used a molecular replacement strategy in which one or more intermolecular interactions were disrupted by domain deletion or point mutagenesis in order to provide insight into the mechanism by which PTP σ signals the formation of a nascent synapse. We find that the ability of PTP σ to mediate the induction of new presynaptic sites through its canonical trans-synaptic partners does not depend on its ability to dephosphorylate targets or to bind HSPGs, but it does require the binding site for liprin- α . Our results also suggest that, contrary to previous reports, binding between PTP σ and liprin- α involves both the D1 and D2 domains of PTP σ .

MATERIALS AND METHODS

DNA Constructs and Viral Vectors

The pFB-shPTP vector used to package AAV6-shPTP was generated based on L315-shCtrlx4 (Gokce and Südhof, 2013), pFB-AAV-GFP-4xshRNA (Zhang et al., 2018), and shRNA sequences against PTP σ (5'-GGCATCATGGGTAGTGATT-3'), PTP δ [5'-GTGCCGGCTAGAACTTGT-3' (Dunah et al., 2005)], and LAR [5'-GGCCTACATAGCTACACAG-3' (Mander et al., 2005)]. This plasmid was packaged into AAV6 by Virovek. AAV6-GFP-4xshRNA called here shCtrl was described previously (Zhang et al., 2018).

The following constructs were described previously: HA-CD4, pLL-CFP (shCtrl-resistant; Zhang et al., 2018), HA-TrkC and TrkC-CFP (both the non-catalytic form; Takahashi et al., 2011). HA-NGL-3 was created based on NGL-3-CFP (Siddiqui et al., 2013) by inserting an HA tag (YPYDVPDYA) following the signal peptide and removing the C-terminal CFP, and V5-CD4 was created from YFP-CD4 (Takahashi et al., 2011) by replacing the YFP tag with V5 (GKPIPPLLGLDST) following the signal peptide.

pLL3.7-hSyn-V5-PTP σ wild-type (WT), ICR deletion (Δ ICR, missing amino acids 974–1530, KLSQ..HYAT), C1142S, 4K4A, D1 deletion (Δ D1, missing amino acids 993–1232, SNLE..EAVG), D2 deletion (Δ D2, missing amino acids 1251–1523, AQVE..EYLG), D2D2 (amino acids 993–1232 replaced by amino acids 1251–1523), PPLL, QFG, and EGFID were generated based on C1-YFP-mouse PTP σ with four FNIII domains and lacking both the meA and meB splice inserts (Takahashi et al., 2011). The V5 tag was inserted directly after the signal peptide and YFP was removed, and the WT construct (which was used as the template to construct all mutants) was made shRNA-resistant by mutating the sequence GGCATCATGGGTAGTGATT to GGaATaATGGGAGcGATT.

C1-myc-trio (Terry-Lorenzo et al., 2016) was a kind gift from Dr Craig Garner (German Center for Neurodegenerative Diseases, Bonn, Germany) and contains the human trio cDNA sequence. Mouse caskin1 cDNA (accession number BC060720) was obtained from Open Biosystems. A small portion of the 5' end of the cDNA was missing and was restored by PCR.

CMV-HA-liprin- α 2 containing the mouse liprin- α 2 gene was a kind gift from Dr. Susanne Schoch (Institute of Neuropathology, Bonn, Germany) containing the mouse liprin- α 2 gene. We mutated the sequence GGGGCTGATCCACCGGAGTTT to GGaGCcGATCCcCaG AaTTT in order to make the sequence resistant to an shRNA (not used in this work) without changing the amino acid sequence. From the resulting plasmid, we transferred the open reading frame to the pBA vector, which contains the CAG chicken β -actin promoter and was a kind gift from Dr Gary Banker (Oregon Health and Sciences University, Portland, OR, USA), and replaced the N-terminal HA tag with a myc tag (EQKLISEEDL) to generate pBA-myc-liprin- α 2.

Fusions with the dihydrofolate reductase (DHFR) F3 C-terminal fragment were made based on p41-HPH-TEF-SspBYGMF-linker-DHFR-F3 (Tarassov et al., 2008). PTP σ , liprin- α 2, caskin1, and trio sequences were subcloned either in full or in truncated form from the plasmids described above so that they were fused at their C-termini *via* a short linker to the F3 fragment. PTP σ ICR consisted of amino acids 974–1530 (KLSQ..HYAT), liprin- α 2 SAM consisted of amino acids 877–1192 (KDRR..SDDK), caskin1 SAM consisted of amino acids 344–636 (AIVK..MAIE), and trio IgPSK consisted of amino acids 2237–3062 (NQRN..LPRV). Fusions with the DHFR F1–2 N-terminal fragment were cloned into the p413 vector (Mumberg et al., 1995). A cassette containing the DHFR F1–2 fragment and the Adh1 terminator from pAG25-F1–2 (Tarassov et al., 2008) was fused to the C-terminus of PTP σ full-length (FL) or ICR under the control of the TEF promoter. PTP σ -FL-DHFR both F1–2 and F3 contained an N-terminal V5 tag. NgCAM, which was a kind gift from Dr Peter Sonderegger (University of Zurich, Zurich, Switzerland), and YFP were each separately fused to F1–2 and to F3 as controls. Point mutations were introduced into PTP σ FL or ICR DHFR F1–2 fusions, and also into the PTP σ FL DHFR F3 fusion in the case of the PPLL mutant (Hofmeyer and Treisman, 2009).

Neuron Culture, Transfection, and AAV Transduction

This study was carried out in accordance with the recommendations of the Canadian Council on Animal Care. The protocol was approved by the University of British Columbia Animal Care Committee.

Primary embryonic day 18 (E18) rat hippocampal neurons were cultured essentially according to the method described in Kaech and Banker (2006). For expression of DNA constructs, the AMAXA nucleofector system (Lonza) was used to deliver an appropriate amount of plasmid (2–4 μ g per construct) to 1–2 million freshly dissociated cells. Cells were plated on poly-L-lysine-coated coverslips at an initial density of approximately 700,000–900,000 for transfected neurons, or 500,000 for untransfected neurons, per 6-cm dish. Neurons were maintained with a glial feeder layer, and cytosine arabinoside (5 μ M) was added at DIV 2 to prevent glial overgrowth. DL-2-amino-5-phosphonovaleric acid (APV, 100 μ M) was added starting from DIV 5 in order to limit excitotoxicity and improve neuronal survival.

Delivery of AAVs was accomplished by incubating DIV 6 neurons face-up in 12-well plates, each well containing 700 μ L of glial-conditioned media with 5×10^9 viral genomes (vg) of the appropriate viral construct. Conditioned media was harvested from either the neurons' own dishes or from similar dishes and was centrifuged for 5 min at $1,500 \times g$ before use. APV was added at a concentration of 100 μ M. Neurons were incubated in the virus-containing solution for 4 h and then transferred back to their home dishes.

Real Time Quantitative PCR (RT-qPCR)

RT-qPCR was performed to confirm triple knockdown of PTP σ , PTP δ , and LAR by AAV6-shPTP. Neurons were treated with AAV carrying shCtrl or shPTP as above, harvested on DIV 16 in cold PBS, and then lysed in TRIzol reagent (Invitrogen). RNA extraction from lysates was performed immediately using the PureLink RNA Mini Kit (Thermo Fisher Scientific). Elimination of genomic DNA and retro-transcription to cDNA were performed using SuperScript IV Vilo Master Mix with ezDNase Enzyme (Thermo Fisher Scientific). SYBRGreen qPCR (PowerUpTM SYBR Green Master Mix, Thermo Fisher Scientific) was performed using the resulting cDNA, with glyceraldehyde-3-phosphate dehydrogenase (GAPDH) and β -actin (Actb) as reference genes. Primers used are listed in the table below, and their efficiency was estimated as between 0.87 and 1.05. All quantitation cycle (Cq) values were detected prior to completion of the 38th cycle.

List of primers used in quantitative RT-PCR assays.

Gene (Rat)	Forward Primer 5'–3'	Reverse Primer 3'–5'
PTP σ	CTTGAGTTCAAGAGGCTTGC	GTCTGTAGCCGTCGATGAAG
PTP δ	CCATGCAGAGTCCAAGATGT	GACAGGACCTACGACCCATA
LAR	CTTCAAGCTCTCTGTTCACTGC	ACCCCGCCTAATGTATAAACG
GAPDH	AGACAAGATGGTGAAGGTCG	TCGTTGATGGCAACAATGTC
Actb	GATCAAGATCATTGCTCCTCCTG	AAGGGTGTAAAACGCAGCTC

Knockdown Confirmation by Western Blot

Neurons were treated with AAV carrying shCtrl or shPTP as above and harvested for Western blotting at DIV 17–18 using Complexiolite-48 (50 μ L/coverslip, Logopharm). Protein concentrations were determined, and equal amounts were run on 10% SDS-polyacrylamide gels. Proteins were blotted using Immobilon P membranes (Millipore). Membranes were blocked using 5% skim milk in Tris-buffered saline with 0.001% Tween-20 and incubated in antibody solution. Primary antibodies used were anti-PTP σ (mouse, 17G7.2, MM-0020, Medimabs) and anti- β -actin (rabbit, 1:5,000, ab8227, Abcam). Secondary antibodies were goat anti-mouse or goat anti-rabbit HRP conjugate from Southern Biotech. Detection was performed using Immobilon Western Chemiluminescent substrate (Millipore).

Coculture Assay

COS cells were maintained in Dulbecco's modified Eagle's medium (DMEM) with 10% bovine growth serum (BGS). When neurons reached the age of DIV 12, near-confluent COS cells were harvested using 0.25% trypsin-EDTA and plated in 12-well plates, then transfected the following day at \sim 85% confluence using polyethylenimine (Boussif et al., 1995) with 1 μ g of plasmid DNA encoding a tagged form of either a postsynaptic organizing protein or CD4 as a non-synaptogenic control. The day after transfection, when neurons were at DIV 13, COS cells were harvested again as before, washed twice with DMEM with 10% BGS, resuspended in glial conditioned media (treated as above for viral infection), and plated at a density of \sim 20,000 cells per coverslip on top of the neurons. Cocultures were allowed to incubate for 18–24 h prior to fixation and staining.

HEK Cell Cultures and Clustering Assay

Maintenance, harvesting, and transfection of HEK 293 (HEK) cells were performed in the same manner as for COS cells, except that the concentration of trypsin-EDTA used was 0.05%. Prior to transfection, cells were plated in 12-well plates on coverslips coated in poly-D-lysine (PDL). The clustering assay was performed by transfecting HEK cells with a mixture of 0.2 μ g of pBA-myc-liprin- α 2, 0.6 μ g of pLL-V5-PTP σ WT or mutant, and 0.2 μ g of pLL CFP. Control coverslips replaced either the liprin- α 2 or the PTP σ plasmid with an equal amount of additional pLL CFP plasmid, such that the total DNA amount was always 1 μ g.

Immunocytochemistry and Imaging

Live surface staining for both HEK cells (Figure 7) and cocultures (Figures 2–4) was performed by incubating coverslips face-up in antibody solution for 30 min on an ice block in a 37°C, 5% CO₂, humidified incubator. Antibody solution was made with fresh Neurobasal media. APV was added at a concentration of 100 μ M for experiments involving neurons. Coverslips were washed with Neurobasal media three times prior to fixation.

Cells were fixed in warm phosphate-buffered saline (PBS) with 4% paraformaldehyde and 4% sucrose for 12 min. Surface staining of V5-PTP σ in neurons was performed after fixation but before permeabilization. For experiments involving surface

staining of both V5-PTP σ and HA, staining was performed after fixation for both antibodies. Non-permeabilized cells were blocked for 30 min in blocking buffer (3% BSA, 5% normal goat serum in PBS) at 37°C, then incubated in primary antibody solution in blocking buffer at 4°C for two nights prior to permeabilization. Cultures were permeabilized using 0.2% Triton-X100 in PBS for 5 min. Cultures were blocked as above and remaining primary antibodies were applied in blocking buffer overnight at 4°C. Secondary antibodies were applied in blocking buffer for 45 min at 37°C.

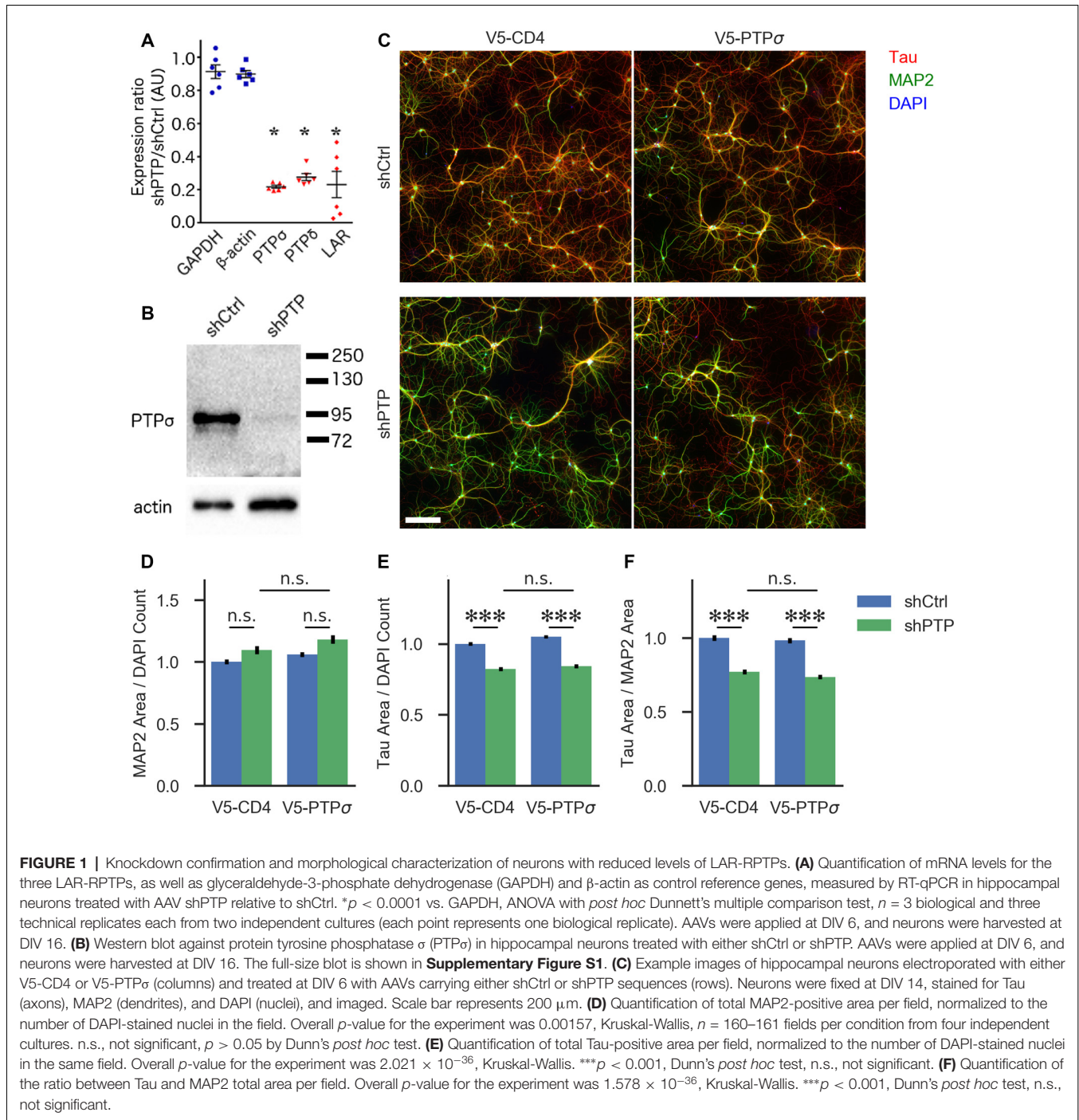
Primary antibodies used were mouse IgG1 anti-SynapsinI (Synaptic Systems, cat no. 106011, 1:40,000, used in Figures 2–4), rabbit anti-SynapsinI (Millipore, cat no. ab5905, 1:10,000, used for all other synapsin staining), mouse IgG2a anti-TauI (Millipore, cat no. PC1C6, 1:2,000), chicken anti-microtubule-associated protein 2 (anti-MAP2; Abcam, cat no. ab5392, 1:2,000), mouse IgG2b anti-HA (Abcam, cat no. 12CA5, 1:500), mouse IgG1 anti-myc (Santa Cruz, cat no. sc-40, 1:500, used in Figure 7) rabbit anti-myc (Sigma, cat no. C3956, 1:2,000, used for all other myc staining), rabbit anti-V5 (Cell Signalling Technology, cat no. 13202, 1:5,000, used in Figure 7 for total V5 staining), and mouse IgG2a anti-V5 (Thermo Fisher, cat no. R960, 1:5,000, used for all V5 surface staining). Secondary antibody against chicken was AMCA AffiniPure Goat Anti-Chicken IgY (IgG; H + L; Jackson, cat no. 103155, 1:200). All other secondary antibodies were from Thermo Fisher and generated in goat, conjugated to Alexa Fluor 488, 568, or 647. Alexa Fluor-conjugated secondary antibodies were used at a concentration of 1:1,000.

Imaging of HEK cells for the co-clustering assay was performed on a Zeiss LSM700 with a 40 \times /1.4 NA oil immersion objective at 2 \times zoom, using single optical sections. Cells were selected based on the channels containing CFP and liprin- α 2 only. Cells without expression of both CFP and liprin- α , as well as cells showing diffuse liprin- α signal, were avoided.

For all other experiments, imaging was performed on either the same microscope in epifluorescence mode or on an Axioplan 2, with either a 10 \times /0.45 NA air (morphology experiments shown in Figure 1) or a 40 \times /1.4 NA oil immersion (all others) objective and a Hamamatsu Orca-Flash4.0 CMOS camera. For experiments imaged using the LSM700, images were acquired as a z-stack containing three slices at 1.46 μ m spacing (10 \times), or 11 slices at 0.23 μ m spacing (40 \times), then combined into a single plane using the Zeiss Extended Depth of Focus module. All imaging was performed blind to experimental condition.

Quantification, Statistical Analysis, and Data Visualization

The order of images was randomized, and measures were performed blind to experimental condition. Images were analyzed in FIJI (NIH) using custom-written Python scripts. Regions of interest (ROIs) were generated by manually choosing a lower brightness threshold for each image and then converting the thresholded image to an ROI using the command "Create Selection." For experiments where measurements were taken from an ROI based on multiple channels, single-channel ROIs were combined using the ROI Manager tool. For coculture



experiments, the ROI based on the MAP2 channel was first dilated by five pixels using the command “Enlarge,” then inverted using “Make Inverse.” The purpose of these two steps was to limit the final ROI to areas of the image which did not contain dendrites and to also exclude the area immediately around the dendrite which could contain spine-associated synapses not directly overlapping the MAP2 signal. In the coculture assay, the threshold for synapsin or myc-liprin- $\alpha 2$ was chosen to include only punctate signal. Thus, the final measure

was punctate synapsin or myc-liprin- $\alpha 2$ per COS cell area or per COS cell axon contact area, all lacking dendrite contact. For the HEK cell co-clustering assay, a background subtraction step was first performed on the myc-liprin- $\alpha 2$ channel using the rolling ball method with a radius of 14 pixels. ROIs were generated by thresholding the CFP cell-fill and background-subtracted myc-liprin- $\alpha 2$ channels. Combined ROIs representing CFP-positive, myc-liprin- $\alpha 2$ -positive; and CFP-positive, myc-liprin- $\alpha 2$ -negative regions were used to measure the surface and

total V5-PTP σ channels. The V5-PTP σ channels were not thresholded. The mean intensity within the first ROI divided by that within the second was used as a measure of the strength of co-clustering.

For experiments in which cells were chosen in order to ensure even surface expression of V5 across conditions, cells showing high or low V5 levels were excluded before analyzing downstream measures such as synapsin intensity.

Analysis of image measurement results and DHFR assay growth data, statistical analysis, and data visualization were performed using Jupyter Notebook (Kluyver et al., 2016), Python 3, and the following packages: pandas, numpy, re, scipy.stats, scikit_posthocs, seaborn, and matplotlib. Data were tested for normality using scipy.stats.normaltest, and analyzed using non-parametric tests as indicated in figure legends if found to be non-normal. Visualization of protein crystal structures was performed using the PyMOL Molecular Graphics System, Version 1.8.6.0 Schrödinger, LLC.

Yeast Cultures and DHFR Assay

Yeast (strain BY4741) were transformed with two plasmids, the first containing DHFR-F1-2 fused to the C-terminus of either PTP σ FL or ICR or a control, and the second containing DHFR-F3 fused to the C-terminus of the indicated interacting protein or a control. DHFR-F3 constructs contained the SAM domains of liprin- α 2 and caskin1, the immunoglobulin-like and protein serine kinase domains (IgPSK) of trio, or the FL version of PTP σ . PTP σ ICR-DHFR-F1-2 was used to test for interactions with trio IgPSK since preliminary experiments (not shown) revealed that the growth rate of yeast transformed with trio IgPSK and PTP σ FL was very low. All other DHFR-F3 constructs were transformed along with PTP σ FL-DHFR-F1-2. Negative controls replaced either the F1-2 or the F3 fusion with a control protein of a similar size. PTP σ FL was replaced by NgCAM. PTP σ ICR, liprin- α 2 SAM, caskin1 SAM, and trio IgPSK were all replaced by YFP. Transformed strains were grown on synthetic defined (SD) media lacking histidine and containing hygromycin (100 μ g/mL) to select for doubly transformed cells.

Transformed strains were grown in SD media lacking histidine and adenine (Michnick et al., 2016) and containing hygromycin overnight at 30°C with shaking, then diluted in a 96-well plate with 200 μ L/well to an OD of 0.05 in the same media containing 1% DMSO with or without 200 μ g/mL methotrexate (MTX). Each plate contained a positive control strain with two WT interacting proteins and two YFP or NgCAM negative controls. Each yeast strain had three replicate wells each with DMSO alone or DMSO + MTX. The plate lid was coated with TritonX-100 (0.05% in 20% ethanol) to minimize condensation, and the cultures were incubated in a BioTek Epoch 2 plate reader at 29–31°C (2° gradient intended to prevent condensation on the plate lid) with OD₆₀₀ readings taken every 10 min at least until the blanked log₂(OD₆₀₀) of all samples reached a value of -2, which generally took between 20 and 30 h.

Data were inspected visually for any wells showing abrupt drops in OD₆₀₀ readings or other abnormalities, and such wells were excluded from the dataset. Data were log₂ transformed.

For each well, the slope of the growth curve in the linear range between log₂(OD₆₀₀) values of -3 and -2 (or between -3 and -2.2 in the case of one experiment) was calculated. For each MTX-containing well, the ratio between that well's slope value and the mean slope value for DMSO-containing wells from the same experiment containing the same strain was calculated. Interaction scores were calculated according to the formula (ratio_x - ratio_{NC})/(ratio_{PC} - ratio_{NC}), where ratio_x, ratio_{NC}, and ratio_{PC} are the MTX/DMSO ratios of the strain of interest, the negative control containing either NgCAM-DHFR-F3 or YFP-DHFR-F3, and the positive control which was PTP σ WT-F1-2 co-transfected with the appropriate WT interacting protein-F3, respectively.

RESULTS

Role of LAR-RPTPs in Neuronal Morphology and Presynaptic Differentiation

First, we assessed the role of the LAR-RPTP family in regulating neuronal morphology in cultured hippocampal neurons. Although this aspect of LAR-RPTP function has been extensively studied in other contexts (Ledig et al., 1999; McLean et al., 2002; Thompson et al., 2003; Chagnon et al., 2004; Sapieha et al., 2005; Siu et al., 2007; Horn et al., 2012; Stoker, 2015) and was not a primary focus of this work, understanding the effects of LAR-RPTP knockdown on outgrowth in our system was necessary for designing experiments focused on their role in synapse formation. To this end, we employed an AAV carrying shRNAs targeting PTP σ , PTP δ , and LAR (shPTP) or carrying four copies of an shRNA targeting GFP (shCtrl) as a control. Infection of primary hippocampal neurons with shPTP reduced levels of all three LAR-RPTPs by 70%–80% compared to shCtrl as assessed by RT-qPCR (**Figure 1A**), and strongly reduced levels of PTP σ as assessed by Western blot (**Figure 1B**). Neurons were fixed at DIV 14 and stained with antibodies against Tau and MAP2 to mark axons and dendrites, respectively (example images shown in **Figure 1C**). We observed a consistent reduction in the area occupied by Tau-positive axons, either alone or as a ratio with MAP2-positive dendrite area, in response to shPTP (**Figures 1E,F**). In order to test the ability of PTP σ to rescue this defect, we transfected neurons with either shRNA-resistant V5-PTP σ or V5-CD4 as a control prior to infection with shCtrl or shPTP. However, this manipulation was not able to rescue the outgrowth phenotype (**Figures 1E,F**; see “Discussion” section). Thus, LAR-RPTPs were required for normal axon outgrowth.

To assess the role of LAR-RPTPs in presynaptic differentiation, we used a neuron-fibroblast coculture assay. When COS cells are transfected with the appropriate postsynaptic organizing protein and then added to primary neuronal cultures, presynaptic differentiation is induced at contact sites by local aggregation of axonal LAR-RPTPs or neurexins (Scheiffele et al., 2000; Takahashi and Craig, 2013). The coculture assay allowed us to control for differences in axon growth by normalizing recruitment of the presynaptic marker synapsin to the axon contact area. Further, in the coculture

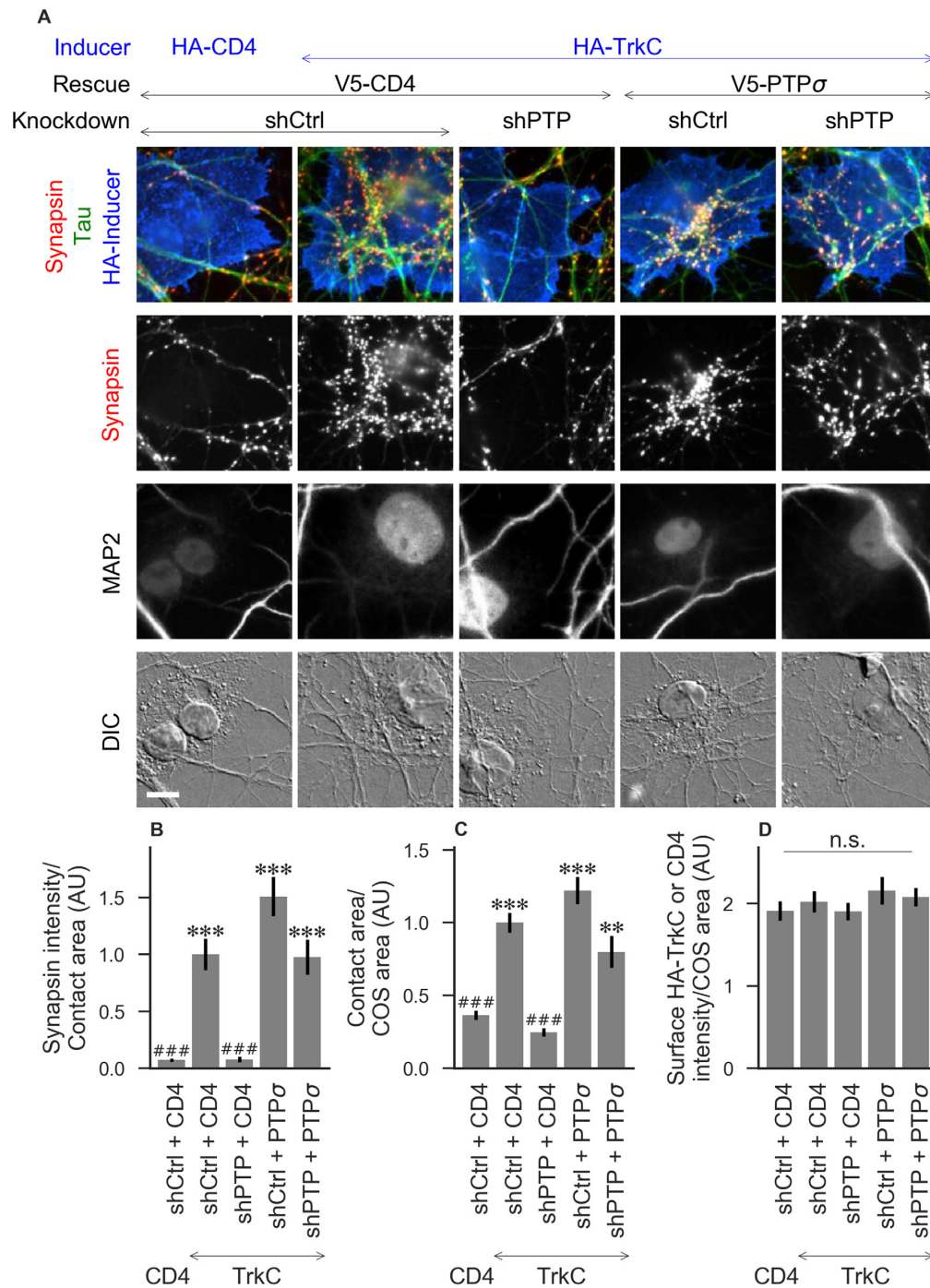


FIGURE 2 | Synaptogenic activity of TrkC is abolished by LAR-RPTP triple knockdown and rescued by PTPσ. **(A)** Representative images of HA-TrkC cocultures in which neurons were treated with either control (shCtrl) or LAR-RPTP triple knockdown (shPTP)-expressing AAVs, and rescued using V5-CD4 as a control or RNAi-resistant V5-PTPσ. Left-most column shows neurons cocultured with COS cells expressing HA-CD4 as a negative control. Rescue constructs were introduced by nucleofection at DIV 0, AAV shRNAs were applied at DIV 6, and coculture assays were performed at DIV 13–14. Synapsin was recruited in tau-positive axons at sites of contact with TrkC-expressing (but not CD4-expressing) COS cells. Microtubule-associated protein 2 (MAP2) labeling of dendrites was used to exclude native synapses from analysis. Scale bar represents 10 μm. **(B–D)** Quantification of synapsin recruitment, contact area between tau-positive axons and transfected COS cells, and intensity of HA-CD4 or HA-TrkC on the COS cell surface, from the experiment shown in **(A)**. “Contact area” is defined as the region where axons contact the inducer-expressing COS cell, excluding the area overlapped by MAP2-positive dendrites. “COS area” also excludes areas of MAP2 overlap. Values are normalized to the mean value in the shCtrl + CD4 with TrkC coculture condition from the same culture. Data are expressed as mean ± SEM. Overall *p*-values were 5.05×10^{-20} **(B)**, 4.02×10^{-19} **(C)**, and 0.66 **(D)**, Kruskal-Wallis, *n* = 28–32 cells per condition from three independent cultures. ****p* < 0.001, ***p* < 0.01 compared to shCtrl + CD4 with CD4 coculture, ###*p* < 0.001 compared to shCtrl + CD4 with TrkC coculture, Dunn’s *post hoc* test, n. s., not significant.

assay, we could isolate presynaptic differentiation induced by LAR-RPTP ligands TrkC and NGL-3 from differentiation induced by neurexin ligands such as neuroligin-2 (NL2). We cocultured neurons treated as above with COS cells expressing HA-tagged CD4, TrkC, NGL-3, or NL2 from DIV 13–14 (example images shown in **Figure 2A** for CD4 and TrkC, **Figure 3A** for NGL-3, and **Figure 4A** for NL2). As expected, the non-synaptogenic molecule CD4 did not induce clustering of synapsin. Under control conditions (V5-CD4 and shCtrl), TrkC induced robust recruitment of synapsin reflecting presynaptic differentiation at sites of contact between the axons and COS cells, and this was abolished by treatment with shPTP. Cultures transfected with V5-PTP σ showed synapsin recruitment when treated with either shCtrl or shPTP, indicating that PTP σ was able to rescue the synaptogenic activity of TrkC (**Figure 2B**). These measures of synapsin recruitment were normalized to axon contact area, reflecting local presynaptic differentiation. Measuring the extent to which axons were recruited to transfected COS cells revealed the same broad trend in that axon recruitment to TrkC-expressing COS cells was reduced by shPTP and largely rescued by expression of V5-PTP σ (**Figure 2C**). Differences in recruitment of axons and in synapsin clustering could not be explained by differences in surface levels of TrkC between conditions (**Figure 2D**). NGL-3 showed similar results as TrkC, although the ability of PTP σ to rescue axon recruitment was somewhat weaker in this case (**Figures 3B–D**). Neurons treated with shPTP + V5-PTP σ and cocultured with NGL-3 did not show significant differences in axon recruitment from either the positive (shCtrl + V5-CD4, cocultured with NGL-3) or the negative (shCtrl + V5-CD4, cocultured with CD4) control. This partial rescue is consistent with NGL-3's dependence on other ligands within the LAR-RPTP family (Kwon et al., 2010). Synaptogenic activity of NL2 as measured by recruitment of synapsin was unaffected by shPTP. There was a slight reduction in axon recruitment by NL2 in shPTP-treated neurons, which was significant compared to the positive control (shCtrl + V5-CD4, cocultured with NL2) in the shPTP + V5-PTP σ condition, consistent with an overall reduction in axon outgrowth as a result of knockdown of LAR-RPTPs (**Figures 4B–D**).

Domain Analysis of PTP σ

We next sought to understand which domains, molecular interaction sites, and enzymatic activities of PTP σ were required for its synaptogenic activity. To do this, we used a molecular replacement strategy in which neurons were treated with shPTP-containing AAV to knock down native PTP σ and rescued with V5-tagged WT or mutant PTP σ , or CD4 as a negative control. In this and all other experiments involving transfection in neurons, shRNA-resistant versions of PTP σ (either WT or mutant) were used. Since the synaptogenic activity of TrkC was abolished by LAR-RPTP knockdown and fully rescued by PTP σ , for this and all subsequent assays to dissect mechanisms of PTP σ -mediated presynaptic differentiation, we used TrkC cocultures.

We hypothesized that, because liprin- α , caskin, and trio all bind to the D2 domain, while there are no known binding partners of the D1 domain aside from PTP σ itself, loss of the

D2 domain would prevent PTP σ from mediating presynaptic differentiation in the coculture assay. We also thought it possible that phosphatase activity against p250GAP, β -catenin, N-cadherin, or an unknown target could be necessary for PTP σ 's synaptogenic activity, meaning that the D1 domain would also be required. Alternatively or in addition, the D1 domain could act as a spacer between the cell membrane and the D2 domain thus allowing D2 to assemble a multi-protein presynaptic complex. Replacing the D1 domain with a second copy of D2 would restore such a steric role for the D1 domain but not a specific catalytic or interaction role. We further asked whether HSPG binding to a co-receptor might be needed for PTP σ 's synaptogenic activity. Thus, we tested the following mutants: a deletion of the entire intracellular region (Δ ICR), a deletion of the D1 or D2 domain (Δ D1 and Δ D2), a mutant in which the D1 domain was replaced with a second copy of D2 (D2D2), a phosphatase-dead point mutant (C1142S; Streuli et al., 1990), and a mutation of the extracellular region known to disrupt binding to HSPGs (4K4A; Aricescu et al., 2002). A schematic view of these mutants is shown in **Figure 5A**.

Consistent with our hypothesis, we found that deletion of the PTP σ D2 domain completely abolished synaptogenic activity in the coculture assay with TrkC (**Figures 5B,C**). Surprisingly, however, we also found that loss of D1 abolished synaptogenic activity, but loss of phosphatase activity *via* the C1142S mutation had no effect. The D2D2 mutation also abolished synaptogenic activity, ruling out the possibility that the effects of the Δ D1 mutation were due to steric effects related to the position of the D2 domain relative to the cell membrane. Finally, we found no effect of the 4K4A mutation, indicating that the synaptogenic activity of PTP σ does not depend on extracellular HSPG binding. These effects were not due to differences in surface expression or local recruitment of the V5-PTP σ mutants since we stained for the extracellular V5 tag and chose fields for analysis based on equal surface levels (**Supplementary Figure S2A**). The lack of activity of the Δ D1 and D2D2 mutants is surprising given the high degree of 3D structural similarity of the wedge and D1 domains with the D2 domain. Aside from a small linker region between the wedge and D1 domain, the combined wedge and D1 structure overlaps almost perfectly with the D2 domain (**Supplementary Figures S2B–D**). Altogether, these data suggest that specific interactions with both the D1 and D2 domains of PTP σ are required for its function in presynaptic differentiation.

Identification of PTP σ Point Mutants to Disrupt Specific Interactions

To further elucidate the mechanisms by which the PTP σ intracellular domain signals the formation of a new presynaptic compartment, we sought to identify mutations that would specifically disrupt the binding of PTP σ to one or another of its known intracellular interaction partners. We chose to use this approach rather than one based on knockdown of each individual interacting protein because it more directly addresses whether binding between PTP σ and the protein of interest is required, which is a different question from whether the interaction partner itself is required. While this work was in progress, it was shown that knockdown of liprin- α 2 and liprin- α 3 reduced the

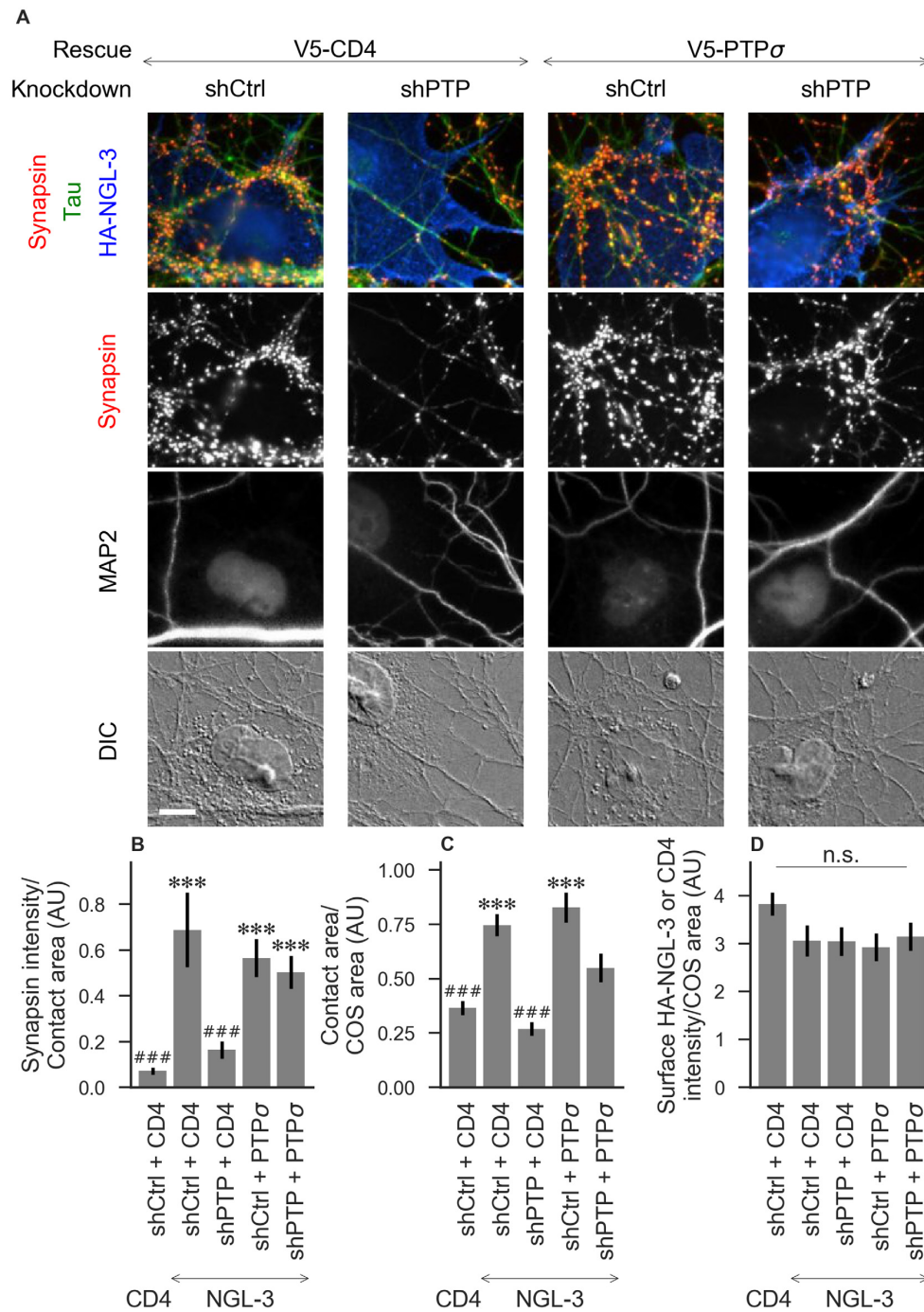


FIGURE 3 | Synaptogenic activity of NGL-3 is abolished by LAR-RPTP triple knockdown and rescued by PTP σ . **(A)** Representative images of HA-NGL-3 cocultures in which neurons were treated with either control (shCtrl) or LAR-RPTP triple knockdown (shPTP)-expressing AAVs, and rescued using V5-CD4 as a control or RNAi-resistant V5-PTP σ . Rescue constructs were introduced by nucleofection at DIV 0, AAV shRNAs were applied at DIV 6, and coculture assays were performed at DIV 13–14. Synapsin was recruited in tau-positive axons at sites of contact with NGL-3-expressing COS cells. MAP2 labeling of dendrites was used to exclude native synapses from analysis. Scale bar represents 10 μ m. **(B–D)** Quantification of synapsin recruitment, contact area between tau-positive axons and transfected COS cells, and intensity of HA-CD4 or HA-NGL-3 on the COS cell surface, from the experiment shown in **(A)**. “Contact area” is defined as the region where axons contact the inducer-expressing COS cell, excluding the area overlapped by MAP2-positive dendrites. “COS area” also excludes areas of MAP2 overlap. Values are normalized to the mean value in the shCtrl + CD4 with TrkC coculture condition from the same culture. Data are expressed as mean \pm SEM. Overall p -values were 6.69×10^{-13} **(B)**, 4.07×10^{-13} **(C)**, and 0.034 **(D)**, although none of the individual comparisons were significant based on Dunn’s *post hoc* test), Kruskal-Wallis, $n = 27$ –31 cells per condition from three independent cultures. *** $p < 0.001$ compared to shCtrl + CD4 with CD4 coculture, ### $p < 0.001$ compared to shCtrl + CD4 with NGL-3 coculture, Dunn’s *post hoc* test. CD4 coculture condition is the same as that shown in **Figure 2** (see **Figure 2A** for example image), n. s., not significant.

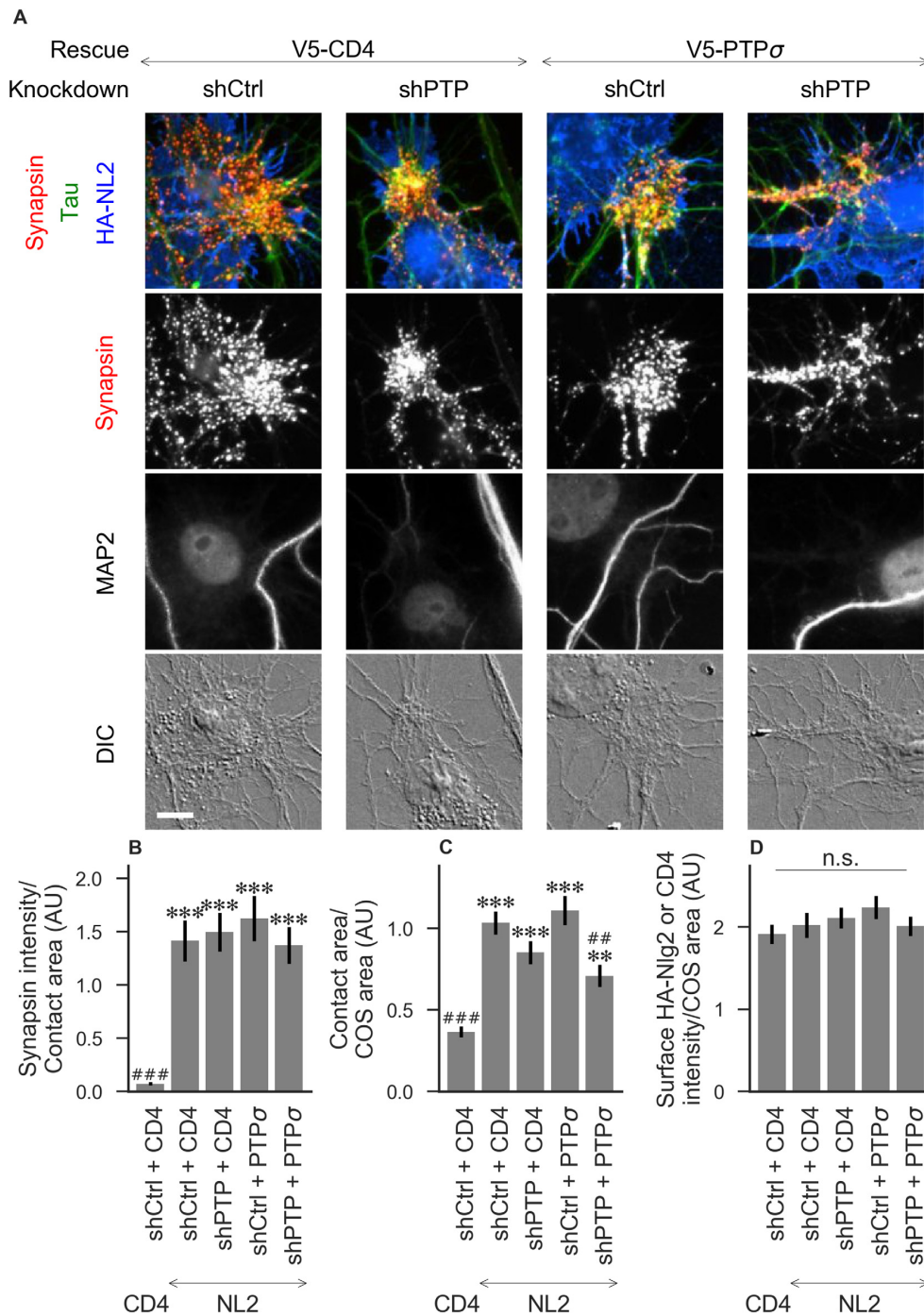


FIGURE 4 | Synaptogenic activity of neuroligin-2 (NL2) is unaffected by LAR-RPTP triple knockdown or expression of PTP σ . **(A)** Representative images of HA-NL2 cocultures in which neurons were treated with either control (shCtrl) or LAR-RPTP triple knockdown (shPTP)-expressing AAVs, and rescued using V5-CD4 as a control or RNAi-resistant V5-PTP σ . Rescue constructs were introduced by nucleofection at DIV 0, AAV shRNAs were applied at DIV 6, and coculture assays were performed at DIV 13–14. Synapsin was recruited in tau-positive axons at sites of contact with NL2-expressing COS cells. MAP2 labeling of dendrites was used to exclude native synapses from analysis. Scale bar represents 10 μ m. **(B–D)** Quantification of synapsin recruitment, contact area between tau-positive axons and transfected COS cells, and intensity of HA-CD4 or HA-NL2 on the COS cell surface, from the experiment shown in **(A)**. “Contact area” is defined as the region where axons contact the inducer-expressing COS cell, excluding the area overlapped by MAP2-positive dendrites. “COS area” also excludes areas of MAP2 overlap. Values are normalized to the mean value in the shCtrl + CD4 with TrkC coculture condition from the same culture. Data are expressed as mean \pm SEM. Overall p -values were 4.70×10^{-15} **(B)**, 2.44×10^{-13} **(C)**, and 0.40 **(D)**, Kruskal-Wallis, $n = 26$ –32 cells per condition from three independent cultures. *** $p < 0.001$, ** $p < 0.01$ compared to shCtrl + CD4 with CD4 coculture, ### $p < 0.001$, ## $p < 0.01$ compared to shCtrl + CD4 with NL2 coculture, Dunn’s *post hoc* test. CD4 coculture condition is the same as that shown in **Figure 2** (see **Figure 2A** for example image), n. s., not significant.

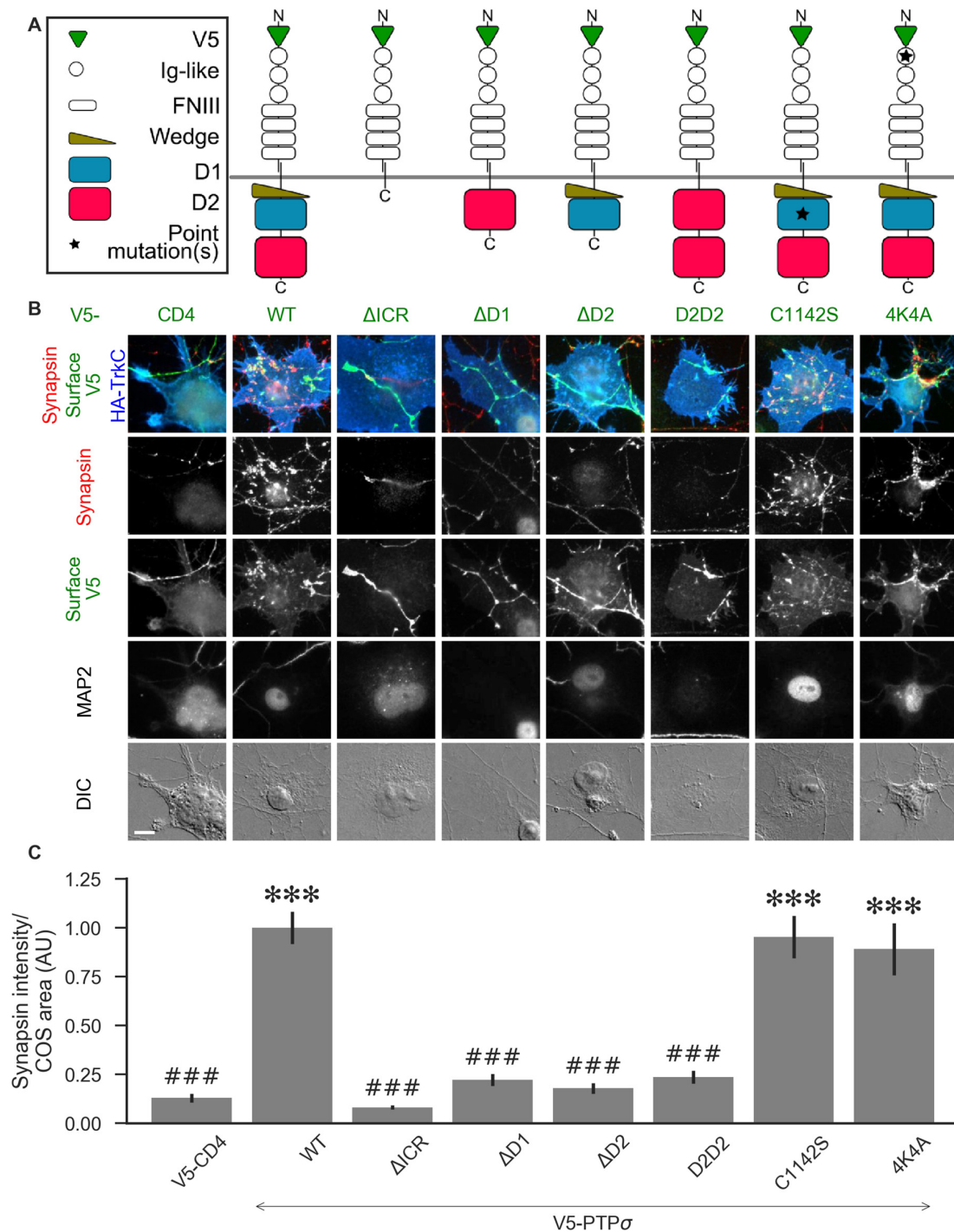


FIGURE 5 | PTP σ requires its D1 and D2 domains, but not its phosphatase activity or heparan sulfate (HS)-binding, to mediate TrkC synaptogenic activity.

(A) Schematic view of PTP σ mutants used in this experiment. Each schematic corresponds to the label and column of images directly below it in **(B)**. **(B)** Representative images of HA-TrkC cocultures where neurons were treated with shPTP-expressing AAVs, and rescued using V5-CD4 as a control or RNAi-resistant V5-PTP σ carrying the indicated mutations. Rescue constructs were introduced by nucleofection at DIV 0, AAV shRNAs were applied at DIV 6, and coculture assays were performed at DIV 13–14. MAP2 labeling of dendrites was used to exclude native synapses from analysis. Scale bar represents 10 μ m. **(C)** Quantification of synapsin recruitment shown in **(B)**. “COS area” indicates only the portion of the TrkC-expressing COS cell not overlapping with MAP2 signal. All values are normalized to the mean of the wild-type (WT) condition from the same culture. Data are expressed as mean \pm SEM. Overall p -value for this experiment was 1.32×10^{-44} , Kruskal-Wallis, $n = 33$ –100 cells per condition from 2–3 cultures. *** $p < 0.001$ compared to CD4, ### $p < 0.001$ compared to WT, Dunn's *post hoc* test. There were no differences in surface levels of the V5-PTP σ mutants (**Supplementary Figure S2A**).

ability of both TrkC and NL2 to induce synapses in the coculture assay (Han et al., 2018). This result is consistent with the hypothesis that direct binding of PTP σ to liprin- α (Serra-Pagès et al., 1995), and indirect binding of neurexin to liprin- α through a mutual binding partner such as CASK (Hata et al., 1996; Olsen et al., 2005) might be a necessary step in the synaptogenic process. However, it is also consistent with alternative models in which liprin- α is either recruited to the synapse *via* other proteins with which it interacts or is required within the neuron but does not need to be recruited to nascent synapses.

We tested 22 candidate mutations consisting of between two and seven amino acids each which were well-conserved at least within mammalian LAR-RPTP family members and in many cases in *C. elegans* and *Drosophila* homologs as well. These candidate mutations were surface-accessible and located close to one another on the protein surface (**Supplementary Figure S3**). We also assayed the PPLL mutation which was previously shown to disrupt PTP σ homodimerization (Hofmeyer and Treisman, 2009). We screened these mutants for their ability to bind to liprin- α 2, caskin1, trio, or to a second molecule of PTP σ . To do this, we used the DHFR protein complementation assay, in which the ability of yeast to grow in the presence of the drug methotrexate (MTX) is dependent on the amount of binding between two putative interacting proteins, each of which is fused to one of two fragments of an MTX-insensitive mutant of the DHFR enzyme (Tarassov et al., 2008; Rochette et al., 2015). We assessed the association of PTP σ or its intracellular domain fused to the DHFR N-terminal fragment with the interacting regions of liprin- α 2, caskin1, and trio, as well as with PTP σ itself, fused to the DHFR C-terminal fragment. Negative control strains were constructed in which one of the two interacting proteins was replaced with either YFP or NgCAM. This maintained a constant size of the DHFR fusion proteins which, consistent with previous reports (Rochette et al., 2015), we found to be important for consistency of the assay. Growth of the resulting strains was measured in media containing either MTX (200 μ g/mL, 1% DMSO) or DMSO alone. For each strain, an interaction score was calculated (see “Materials and Methods” section) such that a score of 0 indicates growth equivalent to that of the negative control strain, and 1 indicates WT growth.

Several mutations (MELEFK, WENNS, KLREMG, and HQYWP) moderately to severely disrupted all interactions tested and thus were considered nonspecific (interaction score <0.3 for at least three out of four ligands, shown in gray in **Figure 6A**). These mutations may disrupt activity in the DHFR assay by affecting protein folding, trafficking, or stability. Once these nonspecific mutations are ignored, mutations affecting binding to liprin- α 2 and caskin1 each form a cluster on the surface of the protein (**Figure 6A**, top row). Binding of PTP σ to liprin- α 2 is partially disrupted (with interaction scores between 0.21 and 0.37) by the closely spaced AEY, DWPE, QVHK, QFG, and MRYE mutations (blue). The caskin1 interaction is abolished completely by the MRYE and EGFID mutations (purple). Mutations on the opposite side of the protein, aside from those which were nonspecific, had minimal effect on binding of either protein to PTP σ (**Figure 6A**, bottom row). These results represent the gross mapping of binding sites on

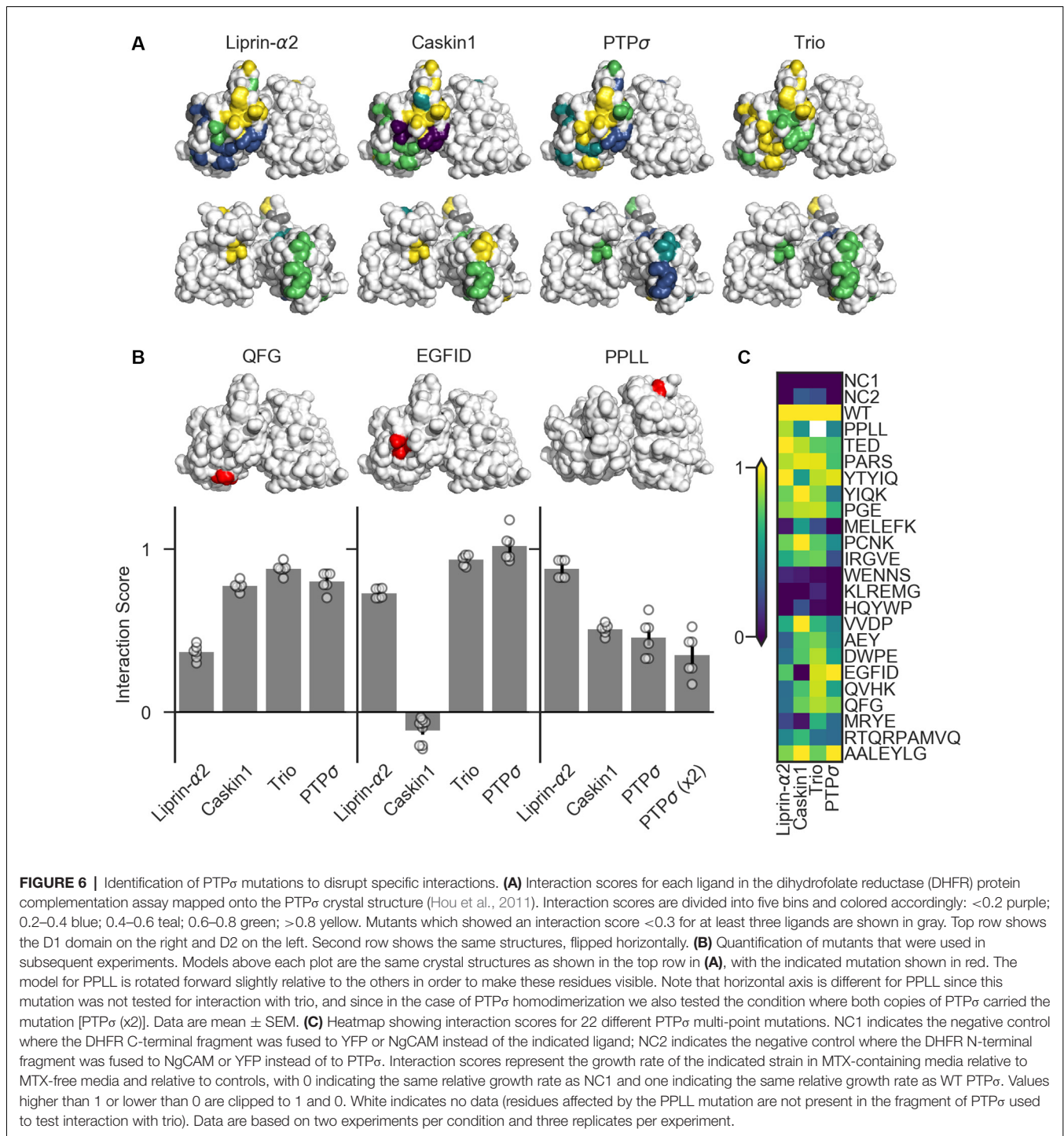
the PTP σ D2 domain for liprin- α 2 and caskin1. The apparent liprin- α 2 binding site on PTP σ constitutes a larger interaction surface than that for caskin1. It is noteworthy that these putative binding sites overlap, suggesting that simultaneous binding of PTP σ to liprin- α 2 and caskin1 may not be possible. Supporting a competitive binding model, LAR is unable to act as a bridge between caskin and liprin- α in yeast two-hybrid assays (Weng et al., 2011). Based on the mutations we tested, clear binding sites were not seen in the D2 domain for PTP σ homodimerization or for trio. For homodimerization, this is not surprising given that binding is thought to be mediated by the wedge domain and the D1 domain (Hofmeyer and Treisman, 2009).

There were several mutations that primarily disrupted binding to liprin- α 2, and of these QFG appeared to be the most specific, with an interaction score of 0.37, compared to between 0.77 and 0.88 for its interaction with caskin1, trio, and PTP σ WT (**Figures 6B,C**). The EGFID mutation is highly effective as well as specific in its disruption of caskin1 binding, with an interaction score of -0.11 for caskin1, and between 0.73 and 1.02 for the other interactions. These two mutations were chosen for further study to determine whether the binding sites on PTP σ for liprin- α , caskin, or both were required for its role in synaptogenesis. The PPLL mutation, which was previously reported to disrupt PTP σ homodimerization only when present on both copies of the protein (Hofmeyer and Treisman, 2009), did indeed disrupt activity in the DHFR assay. In contrast to the previous report, in the DHFR assay, we observed impaired binding between PTP σ WT and PPLL (interaction score of 0.46) as well as between PTP σ PPLL and PPLL (interaction score of 0.35). We also found that this mutation partially disrupts binding to caskin1 (interaction score of 0.51), although not as strongly as EGFID, and does not disrupt binding to liprin- α 2.

Co-clustering of PTP σ Mutants With Liprin- α 2 in HEK Cells

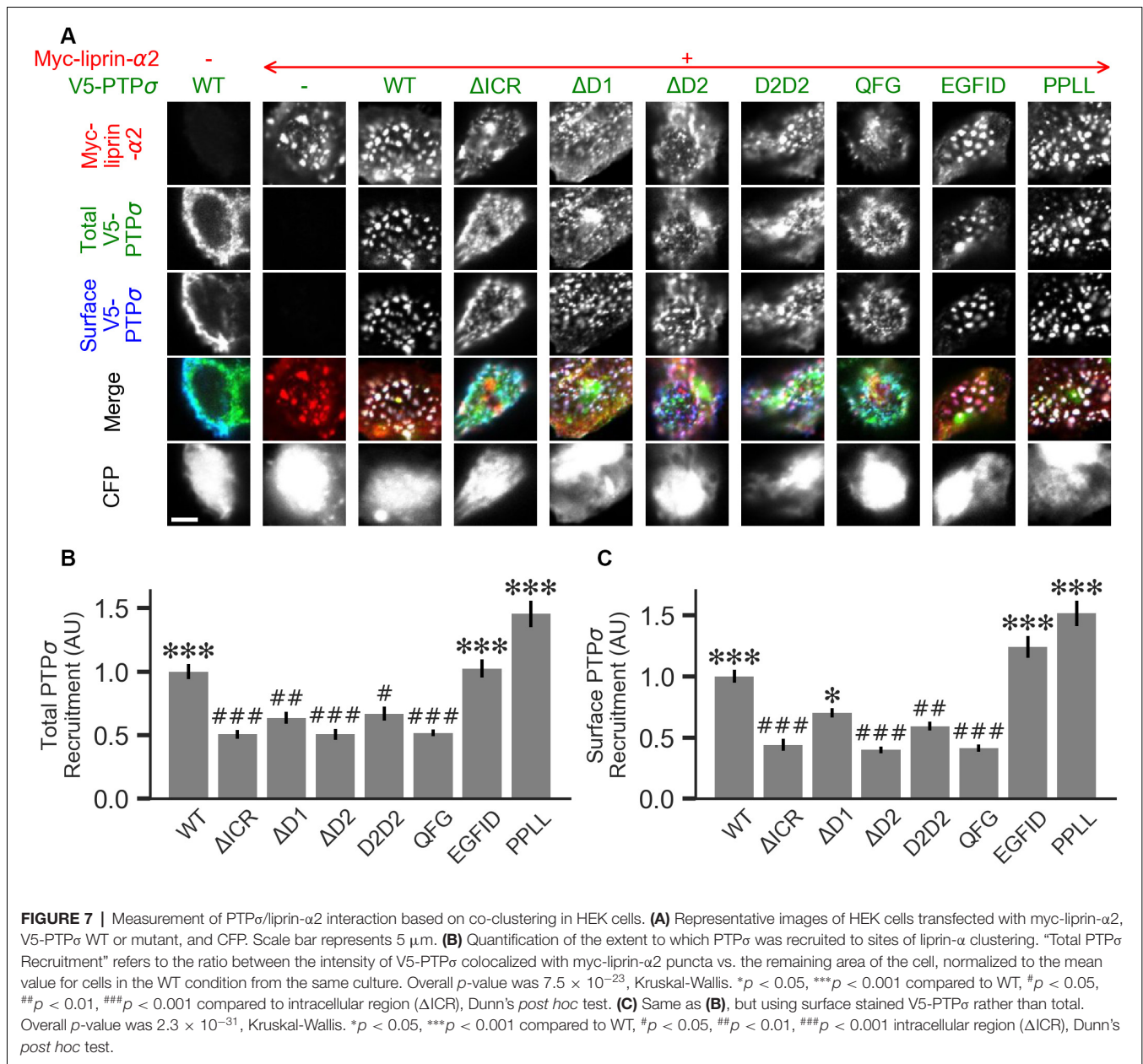
Liprin- α has been previously shown to form clusters when transfected in cell lines and to recruit LAR-RPTPs to these clusters (Serra-Pagès et al., 1998). As a second measure of the interaction strength between the PTP σ mutants and liprin- α 2, we co-transfected myc-liprin- α 2 with V5-PTP σ WT or mutant as well as CFP as a cell fill into HEK 293 cells. In the absence of liprin- α 2, PTP σ was mostly diffuse (**Figure 7A**, left-most column). Consistent with previous reports, liprin- α 2 formed small puncta in some cells when transfected alone (**Figure 7A**, second column from left). When co-transfected with PTP σ , the distribution of liprin- α 2 became more distinctly clustered. Notably, PTP σ was recruited to sites of liprin- α 2 clustering (**Figure 7A**, third column from left). To quantitate these interactions, we calculated a ratio between the intensity of PTP σ fluorescence within the liprin- α 2 patches and that in the remainder of the cell. Analogous experiments were not possible for caskin1, trio, or PTP σ homodimerization because they did not exhibit the same co-clustering phenomenon.

When we transfected HEK cells with liprin- α 2 together with mutant versions of PTP σ , we found that the Δ ICR, Δ D2, and QFG mutants disrupted the co-clustering of the two proteins, such that the distribution of both resembled that seen in



singly-transfected cells. The PPLL and EGFID mutants were essentially unaffected, and the Δ D1 and D2D2 mutants showed a partial disruption of the co-clustering phenomenon. Visually, the liprin- α 2 clusters in cells co-transfected with Δ D1 or D2D2 appeared intermediate between the WT and Δ ICR forms, and the mutant PTP σ was recruited to these patches, though to a lesser extent than with the WT protein. Quantification also revealed an intermediate phenotype. When recruitment

was measured based on total PTP σ staining both Δ D1 and D2D2 were statistically different from WT but not Δ ICR, whereas when surface PTP σ was measured, the Δ D1 mutant was significantly different from Δ ICR but not WT (**Figures 7B,C**). These results are consistent with a model in which binding between liprin- α and PTP σ is mainly mediated by the PTP σ D2 domain as previously reported (Serra-Pagès et al., 1995) and involve the QFG residues, but also involves some contribution



from the D1 domain. Thus, D1 and D2 together mediate full-strength binding of PTP σ to liprin- α .

Recruitment of Liprin- $\alpha 2$ to Nascent Synapses in the Presence of PTP σ Mutants

We predicted that the same PTP σ mutants which disrupted binding to liprin- α in yeast or in HEK cells would also impair recruitment of liprin- α to sites of presynaptic differentiation. To visualize recruitment of liprin- α to presynaptic sites, we transfected neurons with myc-liprin- $\alpha 2$, along with V5-PTP σ , at the time of plating. When we performed cocultures with neurons treated in this manner, we observed significant recruitment of myc-liprin- $\alpha 2$ to COS cells expressing TrkC, compared to those expressing the control protein CD4 (**Figures 8A,B**).

To visualize liprin- α recruitment by PTP σ mutants, we performed additional cocultures in the same manner, except that neurons were treated with shPTP to remove native LAR-RPTs. In addition to WT PTP σ , we tested the Δ D1, Δ D2, D2D2, QFG, EGFID, and PPLL mutants. As in **Figure 5**, we selected cells such that the surface levels of V5-PTP σ were equal across conditions (**Supplementary Figure S2E**). We found that Δ D1, Δ D2, D2D2, and QFG all reduced the extent of liprin- $\alpha 2$ recruitment substantially. Although Δ D1 mediated very weak recruitment, it was significantly higher than that of Δ D2 (**Figures 8C,D**). The level of recruitment by PPLL was similar to WT. Recruitment by EGFID was significantly different from both WT and Δ D2, although it was much closer to WT. These results suggest that direct binding between PTP σ and liprin- α is required

for liprin- α to be recruited to a nascent synapse and that indirect interactions through mutual binding partners are not sufficient.

Synaptogenic Activity of PTP σ Point Mutants

To determine the relative contributions to PTP σ 's synaptogenic activity of the binding interactions between PTP σ and liprin- α , caskin, and itself, we used the QFG, EGFID, and PPLL mutants to rescue activity in the coculture assay. Transfection of shRNA-resistant V5-PTP σ , infection by shPTP, and coculture with HA-TrkC were performed as in **Figure 5**. Fields were selected in order to ensure equal levels of axonal surface V5-PTP σ in contact with the TrkC-expressing COS cells (**Supplementary Figure S2F**), and recruitment of synapsin was measured. We found that the QFG mutation reduced synapsin clustering to levels similar to the Δ ICR mutant (**Figure 9**). In contrast, synapsin clustering by the PPLL and EGFID mutants was not significantly different from WT. Taken together, our results revealed a parallel in the extent of interaction with liprin- α 2 in the yeast and HEK cell assays (**Figures 6, 7**), recruitment of myc-liprin- α 2 in neurons (**Figure 8**), and presynaptic differentiation (**Figures 5, 9**). Thus, binding of PTP σ to liprin- α is likely essential for synaptogenesis induced by the TrkC/PTP σ trans-synaptic complex. In contrast, mutations which disrupt PTP σ homodimerization and binding to caskin had minimal effect on PTP σ -mediated presynaptic differentiation.

DISCUSSION

The results presented here provide insight into the roles of the LAR-RPTP family in presynaptic differentiation. The ability of the TrkC/PTP σ complex to induce new presynaptic sites was not impaired by mutations which disrupted PTP σ homodimerization, phosphatase activity, or binding to HSPGs or to caskin. In contrast, we found that PTP σ -mediated presynaptic differentiation requires liprin- α -binding regions in the PTP σ D2 and D1 domains. While this article was in preparation, Han et al. (2018) reported an overlapping study, but with some important differences. Their findings are consistent with ours regarding the importance of liprin- α but diverge regarding the role of PTP σ 's phosphatase activity.

The LAR-RPTP Family Functions in Axon Growth

We observed a reduction in axon outgrowth by neurons treated with shPTP compared to those treated with shCtrl, with no difference in dendritic outgrowth. The inability of V5-PTP σ to rescue this phenotype could result both from technical factors, such as the electroporation method used, which only targets a portion (~50%) of the cells, or from off-target effects of the shRNA on neuronal process growth. Alternatively, the lack of rescue could result from the fact that we used only a single LAR-RPTP family member. In other words, the reduction in growth might be caused primarily by the loss of LAR and/or PTP δ , rather than by loss of PTP σ . Whereas TrkC-mediated presynaptic differentiation assessed in the other experiments involves only PTP σ (Takahashi et al., 2011), much evidence

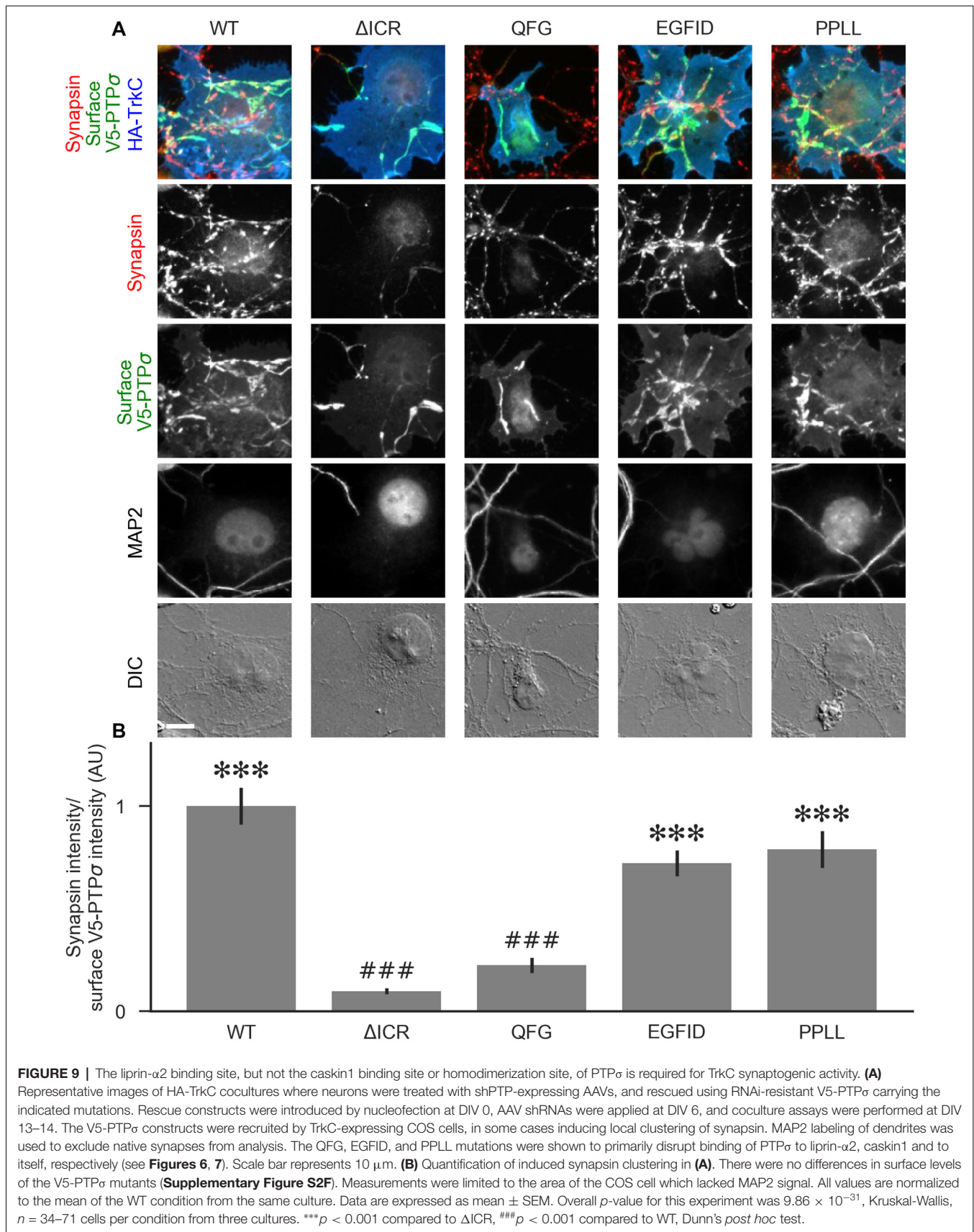
indicates a role of all three LAR-RPTPs in axon outgrowth, targeting, and regeneration (Chagnon et al., 2004; Stoker, 2015). Furthermore, the roles of LAR-RPTPs in regulating axon growth may be context dependent. PTP σ knockout mice have shown accelerated axon outgrowth following nerve injury and in cultures of cortical or dorsal root ganglion neurons (McLean et al., 2002; Thompson et al., 2003; Sapieha et al., 2005; Siu et al., 2007) and increased hippocampal mossy fiber sprouting with aging or seizures (Horn et al., 2012). In contrast, disrupting the function of CRYP α , the chicken homolog of PTP σ , inhibited retinal axon outgrowth (Ledig et al., 1999). Uninjured PTP σ knockout mice show a thinner corpus callosum compared to WT controls, which could indicate defects in either outgrowth or targeting (Meathrel et al., 2002). The extracellular region of PTP σ can bind to both HSPGs and chondroitin sulfate proteoglycans (CSPGs), and its status as an activator or inhibitor of axon outgrowth appears to depend on the local balance of HSPGs and CSPGs (Coles et al., 2011). Interestingly, the extracellular ligand needed for CRYP α -dependent promotion of axon outgrowth, although it was not identified specifically, was determined to come from glial endfeet (Ledig et al., 1999). It is possible that the culture system used in our experiments, in which neurons contact substrates coated with glial-derived factors, results in an environment in which the ligands that PTP σ (and possibly PTP δ and LAR) are exposed to are, on the whole, growth-promoting rather than growth-inhibiting.

Whatever the reason for the reduction in axon outgrowth with shPTP, this change in neuronal morphology would complicate the interpretation of many assays for native synapses. Any potential reductions in synapse density could result from either a reduction in axon/dendrite contacts as a result of reduced axon length overall, or from specific roles of the LAR-RPTPs in local differentiation of contacts into functional synapses. Thus, the reductions in synapse density and in the frequency of miniature synaptic currents reported with knock-down of LAR-RPTPs in hippocampal cultures (Han et al., 2018) could reflect deficits in axon outgrowth and/or in synapse development.

Effects of the shPTP treatment on axon outgrowth were also apparent in the diminished level of axon recruitment in the coculture experiments. Expression of shRNA-resistant V5-PTP σ partially rescued axon recruitment, to a greater extent for cells expressing TrkC than NGL-3 or NL2. In the statistical analyses, axon recruitment was significantly diminished in the shPTP knockdown and PTP σ rescue group compared with the shCtrl group only for NL2 and not for TrkC or NGL-3. Considering that NL2 is not a LAR-RPTP ligand, these effects on axon recruitment in coculture are likely due to the effects of shPTP treatment on axon growth in general. Thus to specifically assay synaptogenic activity, we controlled for differences in axon recruitment in the coculture assays.

Role of LAR-RPTPs in Synaptogenesis

We found that LAR-RPTP knockdown abolished the synaptogenic coculture activity of both TrkC and NGL-3 almost entirely, whereas there was no effect on the activity of the neurexin ligand NL2. Our findings contrast with those of another recent study, which found no effect on coculture with NGL-3 in



response to knockdown of any or all of the LAR-RPTPs (Han et al., 2018). It could be that NGL-3's activity requires a fairly low threshold amount of LAR-RPTPs and that the extent of knockdown differed between the two studies. The finding that loss of the LAR-RPTPs is sufficient to abolish NGL-3 activity is consistent with the observation that NGL-3 binds to all three LAR-RPTP family members (Kwon et al., 2010) and has no other known extracellular binding partners. In the case of TrkC, we observed an increase in clustering of synapsin in response to transfection with V5-PTP σ relative to control V5-CD4, although this difference was not significant. This could indicate that the total level of LAR-RPTPs in untreated neurons is not saturating with respect to presynaptic differentiation induced by TrkC.

Despite compelling evidence for a central role of LAR-RPTPs in synaptogenesis in invertebrate systems (Kaufmann et al., 2002; Ackley et al., 2005), assessing their roles in native synaptogenesis in mammals has been more difficult, confounded in part by their roles in axon growth. Mice lacking PTP σ show increased hippocampal synapse density which may be related to increased axon growth (Horn et al., 2012). Importantly, these PTP σ deficient mice also show differences in synapse properties, including elevated paired-pulse facilitation suggesting a reduced probability of release, and reduced long term potentiation (Horn et al., 2012). TrkC-PTP σ and NGL-3-LAR-RPTP complexes may contribute to these synapse properties, and potentially to synapse density as indicated by deficits upon knockdown of TrkC or NGL-3 (Woo et al., 2009; Takahashi et al., 2011).

Domain Requirements for Liprin- α Binding to PTP σ

Since no binding partners of the D1 domain besides PTP σ itself are known, our initial hypothesis was that the D1 domain would either be dispensable for synaptogenic activity or would be required for its phosphatase activity or for homodimerization. The finding that the Δ D1 mutation abolished coculture activity, but the C1142S phosphatase-dead and PPLL non-homodimerizing mutations had no effect, was surprising. Another hypothesis which we considered was that the D1 domain was not required for any catalytic or binding function, but instead acted as a spacer which positioned the D2 domain some distance from the plasma membrane, allowing for the formation of multi-protein complexes required for synapse formation. This hypothesis also turned out to be incorrect, as the D2D2 mutation in which the D1 domain was replaced by a second copy of the similarly-sized D2 domain also abolished activity. Thus, it appeared that the D1 domain must be performing some function which was previously unknown. One clue to this puzzle came from the fact that the Δ D1 mutant surprisingly showed a phenotype intermediate between WT and Δ ICR when we tested its ability to co-cluster with liprin- α 2 in HEK cells. Similarly, replacement of the D1 domain by a second D2 domain (D2D2) disrupted the ability of PTP σ to co-cluster with liprin- α 2 in HEK cells. Furthermore, the Δ D1 and D2D2 mutants were deficient at recruiting liprin- α 2 to TrkC-induced presynaptic sites in neurons. Our data are consistent with a model in which binding to liprin- α 2 is primarily mediated by the D2 domain of PTP σ , but the D1 domain is required for full-strength binding.

Binding between LAR and liprin- α was previously reported to be mediated by the D2 domain, based on the observation that the isolated D2 domain but not the isolated D1 domain showed interaction with liprin- α in a yeast two-hybrid assay (Serra-Pagès et al., 1995). However, this does not rule out the possibility that D1 contributes to the strength of the interaction.

PTP σ -Liprin- α Interaction in Presynaptic Differentiation

A major aim of this study was to examine the downstream pathways and mechanisms which might mediate the synaptogenic effects of PTP σ 's interactions with its postsynaptic ligands. To test the functional relevance of PTP σ 's ability to bind liprin- α , caskin, and itself, we employed a series of point mutants identified using a protein complementation assay. Unfortunately, we were not able to test the importance of a third D2-interacting protein, trio, using this strategy because we did not find any appropriate point mutants. This experiment pointed to liprin- α as the likely most important downstream interacting partner of PTP σ . The QFG mutant, which was able to bind caskin and to homodimerize with PTP σ WT, but not bind liprin- α , almost completely abolished coculture activity. The EGFID and PPLL mutants, which disrupted caskin binding and homodimerization respectively, had mild if any effects.

Our results agree with those of Han et al. (2018) in identifying liprin- α as a likely mediator of PTP σ 's synaptogenic effects. If binding between PTP σ and liprin- α is required, one would expect that both proteins themselves would be necessary for PTP σ -mediated synaptogenesis. Han et al. (2018) found that knockdown of either PTP σ or of liprin- α 2 and - α 3 impaired the ability of PTP σ ligands to induce synaptogenesis in the coculture assay. Our work corroborates and extends upon this finding by providing evidence that not only are LAR-RPTPs and liprin- α required for synaptogenesis but that these two proteins must be able to bind one another.

We did not find any effect of the extracellular 4K4A mutation on coculture activity, indicating that PTP σ 's ability to bind HSPGs is not required for its synaptogenic effects, at least when triggered by binding to TrkC. Homodimerization *via* the ICR of PTP σ also appeared to be dispensable, based on the ability of the non-homodimerizing PPLL mutant to induce clustering of both liprin- α 2 and synapsin. However, this does not preclude the possibility that indirect multimerization of PTP σ might be necessary. The PTP δ postsynaptic ligand SALM5 has been shown to induce formation of tetramers containing two molecules each of PTP δ and SALM5, independently of any direct interactions between PTP δ molecules (Goto-Ito et al., 2018; Lin et al., 2018).

We also found no effect of the phosphatase-dead C1142S mutant on coculture activity of TrkC, indicating that dephosphorylation of targets is not necessary for PTP σ to mediate presynaptic differentiation. In contrast to this finding, Han et al. (2018) reported that the same mutation (C1157S in their PTP σ construct) impairs or abolishes coculture activity of Slitrk1 and TrkC. Two potentially important methodological differences between our study and Han et al. (2018) may contribute to these differences in findings. First, we assessed coculture regions with equal surface expression of the various

PTP σ constructs, as differences in surface trafficking could confound measures of presynaptic differentiation. Second, we excluded native synapses (synapsin puncta associated with MAP2-positive dendrites) from our measures and quantified only presynaptic sites induced by contact with TrkC-expressing cells. This issue may be particularly significant given the finding that PTP σ phosphatase activity regulates native synapse density in hippocampal cultures through a postsynaptic mechanism (Dunah et al., 2005).

In summary, our results indicate that liprin- α binding is likely required for PTP σ -mediated presynaptic differentiation, and that caskin binding, homodimerization, phosphatase activity, and HSPG binding are all dispensable. We cannot be certain that the PTP σ mutations used in our molecular replacement experiments did not disrupt multiple interactions, including potentially those with as yet unidentified binding partners of PTP σ . However, the correspondence between those mutations which disrupted binding to liprin- α in yeast and/or HEK cells and those which abolished recruitment of both liprin- α 2 itself and synapsin in the coculture assay is consistent with the hypothesis that binding to liprin- α is necessary for PTP σ to induce presynaptic differentiation.

DATA AVAILABILITY

The raw data supporting the conclusions of this manuscript will be made available by the authors, without undue reservation, to any qualified researcher. The datasets generated for this study are available on request to the corresponding author.

ETHICS STATEMENT

This study was carried out in accordance with the recommendations of the Canadian Council on Animal Care. The

REFERENCES

- Ackley, B. D., Harrington, R. J., Hudson, M. L., Williams, L., Kenyon, C. J., Chisholm, A. D., et al. (2005). The two isoforms of the *Caenorhabditis elegans* leukocyte-common antigen related receptor tyrosine phosphatase PTP-3 function independently in axon guidance and synapse formation. *J. Neurosci.* 25, 7517–7528. doi: 10.1523/JNEUROSCI.2010-05.2005
- Aricescu, A. R., McKinnell, I. W., Halfter, W., and Stoker, A. W. (2002). Heparan sulfate proteoglycans are ligands for receptor protein tyrosine phosphatase σ . *Mol. Cell. Biol.* 22, 1881–1892. doi: 10.1128/mcb.22.6.1881-1892.2002
- Astigarraga, S., Hofmeyer, K., Farajian, R., and Treisman, J. E. (2010). Three *Drosophila* liprins interact to control synapse formation. *J. Neurosci.* 30, 15358–15368. doi: 10.1523/JNEUROSCI.1862-10.2010
- Boussif, O., Lezoualc'h, F., Zanta, M. A., Mergny, M. D., Scherman, D., Demeneix, B., et al. (1995). A versatile vector for gene and oligonucleotide transfer into cells in culture and *in vivo*: polyethylenimine. *Proc. Natl. Acad. Sci. U S A* 92, 7297–7301. doi: 10.1073/pnas.92.16.7297
- Chagnon, M. J., Uetani, N., and Tremblay, M. L. (2004). Functional significance of the LAR receptor protein tyrosine phosphatase family in development and diseases. *Biochem. Cell Biol.* 82, 664–675. doi: 10.1139/o04-120
- Chagnon, M. J., Wu, C., Nakazawa, T., Yamamoto, T., Noda, M., Blanchetot, C., et al. (2010). Receptor tyrosine phosphatase sigma (RTP σ) regulates p250GAP, a novel substrate that attenuates Rac signaling. *Cell. Signal.* 22, 1626–1633. doi: 10.1016/j.cellsig.2010.06.001

protocol was approved by the University of British Columbia Animal Care Committee.

AUTHOR CONTRIBUTIONS

CB and AC conceived the project and wrote the article with assistance from all authors. NP, BK, and TS performed confirmation of viral-mediated knockdowns and YG did some preliminary characterization. CB generated and analyzed all other data. CL and JC provided expertise and training for the yeast DHFR assay.

FUNDING

This work was supported by Canadian Institutes of Health Research FDN 143206 and Canada Research Chair Awards (to AC), a Natural Sciences and Engineering Research Council of Canada Discovery Grant RGPIN-2015-05994 and Canadian Institutes of Health Research Grant MOP-142209 (to TS), and Faculty of Graduate Studies, University of British Columbia Four-Year Fellowship (to CB).

ACKNOWLEDGMENTS

We thank Xiling Zhou for excellent technical assistance. A version of this work appears in CB's thesis in the University of British Columbia repository, available at <http://hdl.handle.net/2429/69744>.

SUPPLEMENTARY MATERIAL

The Supplementary Material for this article can be found online at: <https://www.frontiersin.org/articles/10.3389/fnsyn.2019.00017/full#supplementary-material>

- Coles, C. H., Mitakidis, N., Zhang, P., Elegheert, J., Lu, W., Stoker, A. W., et al. (2014). Structural basis for extracellular cis and trans RPTP σ signal competition in synaptogenesis. *Nat. Commun.* 5:5209. doi: 10.1038/ncomms6209
- Coles, C. H., Shen, Y., Tenney, A. P., Siebold, C., Sutton, G. C., Lu, W., et al. (2011). Proteoglycan-specific molecular switch for RPTP σ clustering and neuronal extension. *Science* 332, 484–488. doi: 10.1126/science.1200840
- Debant, A., Serra-Pagès, C., Seipel, K., O'Brien, S., Tang, M., Park, S. H., et al. (1996). The multidomain protein Trio binds the LAR transmembrane tyrosine phosphatase, contains a protein kinase domain and has separate rac-specific and rho-specific guanine nucleotide exchange factor domains. *Proc. Natl. Acad. Sci. U S A* 93, 5466–5471. doi: 10.1073/pnas.93.11.5466
- Dunah, A. W., Hueske, E., Wyszynski, M., Hoogenraad, C. C., Jaworski, J., Pak, D. T., et al. (2005). LAR receptor protein tyrosine phosphatases in the development and maintenance of excitatory synapses. *Nat. Neurosci.* 8, 458–467. doi: 10.1038/nn1416
- Gokce, O., and Südhof, T. C. (2013). Membrane-tethered monomeric neuroligin LNS-domain triggers synapse formation. *J. Neurosci.* 33, 14617–14628. doi: 10.1523/JNEUROSCI.1232-13.2013
- Goto-Ito, S., Yamagata, A., Sato, Y., Uemura, T., Shiroshima, T., Maeda, A., et al. (2018). Structural basis of trans-synaptic interactions between PTP δ and SALMs for inducing synapse formation. *Nat. Commun.* 9:269. doi: 10.1038/s41467-017-02417-z
- Graf, E. R., Zhang, X., Jin, S. X., Linhoff, M. W., and Craig, A. M. (2004). Neuroligins induce differentiation of GABA and glutamate postsynaptic specializations *via* neuroligins. *Cell* 119, 1013–1026. doi: 10.1016/j.cell.2004.11.035

- Han, K. A., Ko, J. S., Pramanik, G., Kim, J. Y., Tabuchi, K., Um, J. W., et al. (2018). PTP σ drives excitatory presynaptic assembly *via* various extracellular and intracellular mechanisms. *J. Neurosci.* 38, 6700–6721. doi: 10.1523/JNEUROSCI.0672-18.2018
- Hata, Y., Butz, S., and Südhof, T. C. (1996). CASK: a novel dlg/PSD95 homolog with an N-terminal calmodulin-dependent protein kinase domain identified by interaction with neuroligins. *J. Neurosci.* 16, 2488–2494. doi: 10.1523/JNEUROSCI.16-08-02488.1996
- Hofmeyer, K., and Treisman, J. E. (2009). The receptor protein tyrosine phosphatase LAR promotes R7 photoreceptor axon targeting by a phosphatase-independent signaling mechanism. *Proc. Natl. Acad. Sci. U S A* 106, 19399–19404. doi: 10.1073/pnas.0903961106
- Horn, K. E., Xu, B., Gobert, D., Hamam, B. N., Thompson, K. M., Wu, C., et al. (2012). Receptor protein tyrosine phosphatase sigma regulates synapse structure, function and plasticity. *J. Neurochem.* 122, 147–161. doi: 10.1111/j.1471-4159.2012.07762.x
- Hou, L., Wang, J., Zhou, Y., and Li, J., Zang, Y., Li, J. (2011). Structural insights into the homology and differences between mouse protein tyrosine phosphatase-sigma and human protein tyrosine phosphatase-sigma. *Acta Biochim. Biophys. Sin.* 43, 977–988. doi: 10.1093/abbs/gmr095
- Kaech, S., and Banker, G. (2006). Culturing hippocampal neurons. *Nat. Protoc.* 1, 2406–2415. doi: 10.1038/nprot.2006.356
- Kaufmann, N., DeProto, J., Ranjan, R., Wan, H., and Van Vactor, D. (2002). *Drosophila* liprin- α and the receptor phosphatase Dlar control synapse morphogenesis. *Neuron* 34, 27–38. doi: 10.1016/s0896-6273(02)00643-8
- Kluyver, T., Ragan-Kelley, B., Pérez, F., Granger, B., Bussonnier, M., Frederic, J., et al. (2016). “Jupyter notebooks—a publishing format for reproducible computational workflows,” in *Proceedings of the 20th International Conference on Electronic Publishing* (Gottingen), 87–90. doi: 10.3233/978-1-61499-649-1-87
- Ko, J., Na, M., Kim, S., Lee, J., and Kim, E. (2003). Interaction of the ERC family of RIM-binding proteins with the liprin- α family of multidomain proteins. *J. Biol. Chem.* 278, 42377–42385. doi: 10.1074/jbc.m307561200
- Ko, J. S., Pramanik, G., Um, J. W., Shim, J. S., Lee, D., Kim, K. H., et al. (2015). PTP σ functions as a presynaptic receptor for the glypican-4/LRRTM4 complex and is essential for excitatory synaptic transmission. *Proc. Natl. Acad. Sci. U S A* 112, 1874–1879. doi: 10.1073/pnas.1410138112
- Kwon, S.-K., Woo, J., Kim, S. Y., Kim, H., and Kim, E. (2010). Trans-synaptic adhesions between netrin-G ligand-3 (NGL-3) and receptor tyrosine phosphatases LAR, protein-tyrosine phosphatase δ (PTP δ), and PTP σ *via* specific domains regulate excitatory synapse formation. *J. Biol. Chem.* 285, 13966–13978. doi: 10.1074/jbc.M109.061127
- Ledig, M. M., Haj, F., Bixby, J. L., Stoker, A. W., and Mueller, B. K. (1999). The receptor tyrosine phosphatase CRYPA promotes intraretinal axon growth. *J. Cell Biol.* 147, 375–388. doi: 10.1083/jcb.147.2.375
- Li, Y., Zhang, P., Choi, T.-Y., Park, S. K., Park, H., Lee, E.-J., et al. (2015). Splicing-dependent trans-synaptic SALM3-LAR-RPTP interactions regulate excitatory synapse development and locomotion. *Cell Rep.* 12, 1618–1630. doi: 10.1016/j.celrep.2015.08.002
- Lin, Z., Liu, J., Ding, H., Xu, F., and Liu, H. (2018). Structural basis of SALM5-induced PTP δ dimerization for synaptic differentiation. *Nat. Commun.* 9:268. doi: 10.1038/s41467-017-02414-2
- Mah, W., Ko, J., Nam, J., Han, K., Chung, W. S., and Kim, E. (2010). Selected SALM (synaptic adhesion-like molecule) family proteins regulate synapse formation. *J. Neurosci.* 30, 5559–5568. doi: 10.1523/JNEUROSCI.4839-09.2010
- Mander, A., Hodgkinson, C. P., and Sale, G. J. (2005). Knock-down of LAR protein tyrosine phosphatase induces insulin resistance. *FEBS Lett.* 579, 3024–3028. doi: 10.1016/j.febslet.2005.04.057
- McLean, J., Batt, J., Doering, L. C., Rotin, D., and Bain, J. R. (2002). Enhanced rate of nerve regeneration and directional errors after sciatic nerve injury in receptor protein tyrosine phosphatase σ knock-out mice. *J. Neurosci.* 22, 5481–5491. doi: 10.1523/JNEUROSCI.22-13-05481.2002
- Meathrel, K., Adamek, T., Batt, J., Rotin, D., and Doering, L. C. (2002). Protein tyrosine phosphatase σ -deficient mice show aberrant cytoarchitecture and structural abnormalities in the central nervous system. *J. Neurosci.* Res. 70, 24–35. doi: 10.1002/jnr.10382
- Michnick, S. W., Levy, E. D., Landry, C. R., Kowarzyk, J., and Messier, V. (2016). The dihydrofolate reductase protein-fragment complementation assay: a survival-selection assay for large-scale analysis of protein-protein interactions. *Cold Spring Harb. Protoc.* 2016. doi: 10.1101/pdb.prot090027
- Müller, T., Choidas, A., Reichmann, E., and Ullrich, A. (1999). Phosphorylation and free pool of β -catenin are regulated by tyrosine kinases and tyrosine phosphatases during epithelial cell migration. *J. Biol. Chem.* 274, 10173–10183. doi: 10.1074/jbc.274.15.10173
- Mumberg, D., Müller, R., and Funk, M. (1995). Yeast vectors for the controlled expression of heterologous proteins in different genetic backgrounds. *Gene* 156, 119–122. doi: 10.1016/0378-1119(95)00037-7
- Olsen, O., Moore, K. A., Fukata, M., Kazuta, T., Trinidad, J. C., Kauer, F. W., et al. (2005). Neurotransmitter release regulated by a MALS-liprin- α presynaptic complex. *J. Cell Biol.* 170, 1127–1134. doi: 10.1083/jcb.200503011
- Rochette, S., Diss, G., Filteau, M., Leducq, J.-B., Dubé, A. K., and Landry, C. R. (2015). Genome-wide protein-protein interaction screening by protein-fragment complementation assay (PCA) in living cells. *J. Vis. Exp.* 97:e52255. doi: 10.3791/52255
- Sapieha, P. S., Duplan, L., Uetani, N., Joly, S., Tremblay, M. L., Kennedy, T. E., et al. (2005). Receptor protein tyrosine phosphatase sigma inhibits axon regrowth in the adult injured CNS. *Mol. Cell. Neurosci.* 28, 625–635. doi: 10.1016/j.mcn.2004.10.011
- Scheiffele, P., Fan, J., Choih, J., Fetter, R., and Serafini, T. (2000). Neuroligin expressed in nonneuronal cells triggers presynaptic development in contacting axons. *Cell* 101, 657–669. doi: 10.1016/s0092-8674(00)80877-6
- Schoch, S., Castillo, P. E., Jo, T., Mukherjee, K., Geppert, M., Wang, Y., et al. (2002). RIM1 α forms a protein scaffold for regulating neurotransmitter release at the active zone. *Nature* 415, 321–326. doi: 10.1038/415321a
- Serra-Pagès, C., Kedersha, N. L., Fazikas, L., Medley, Q., Debant, A., and Streuli, M. (1995). The LAR transmembrane protein tyrosine phosphatase and a coiled-coil LAR-interacting protein co-localize at focal adhesions. *EMBO J.* 14, 2827–2838. doi: 10.1002/j.1460-2075.1995.tb07282.x
- Serra-Pagès, C., Medley, Q. G., Tang, M., Hart, A., and Streuli, M. (1998). Liprins, a family of LAR transmembrane protein-tyrosine phosphatase-interacting proteins. *J. Biol. Chem.* 273, 15611–15620. doi: 10.1074/jbc.273.25.15611
- Shen, Y., Tenney, A. P., Busch, S. A., Horn, K. P., Cuascat, F. X., Liu, K., et al. (2009). PTP σ is a receptor for chondroitin sulfate proteoglycan, an inhibitor of neural regeneration. *Science* 326, 592–596. doi: 10.1126/science.1178310
- Siddiqui, T. J., Tari, P. K., Connor, S. A., Zhang, P., Dobie, F. A., She, K., et al. (2013). An LRRTM4-HSPG complex mediates excitatory synapse development on dentate gyrus granule cells. *Neuron* 79, 680–695. doi: 10.1016/j.neuron.2013.06.029
- Siu, R., Fladd, C., and Rotin, D. (2007). N-cadherin is an *in vivo* substrate for protein tyrosine phosphatase sigma (PTP σ) and participates in PTP σ -mediated inhibition of axon growth. *Mol. Cell. Biol.* 27, 208–219. doi: 10.1128/mcb.00707-06
- Spangler, S. A., Jaarsma, D., de Graaff, E., Wulf, P. S., Akhmanova, A., and Hoogenraad, C. C. (2011). Differential expression of liprin- α family proteins in the brain suggests functional diversification. *J. Comp. Neurol.* 519, 3040–3060. doi: 10.1002/cne.22665
- Spangler, S. A., Schmitz, S. K., Kevenaar, J. T., de Graaff, E., de Wit, H., Demmers, J., et al. (2013). Liprin- α 2 promotes the presynaptic recruitment and turnover of RIM1/CASK to facilitate synaptic transmission. *J. Cell Biol.* 201, 915–928. doi: 10.1083/jcb.201301011
- Stoker, A. W. (2015). RPTPs in axons, synapses and neurology. *Semin. Cell Dev. Biol.* 37, 90–97. doi: 10.1016/j.semcdb.2014.09.006
- Streuli, M., Krueger, N. X., Thai, T., Tang, M., and Saito, H. (1990). Distinct functional roles of the two intracellular phosphatase like domains of the receptor-linked protein tyrosine phosphatases LCA and LAR. *EMBO J.* 9, 2399–2407. doi: 10.1002/j.1460-2075.1990.tb07415.x
- Südhof, T. C. (2018). Towards an understanding of synapse formation. *Neuron* 100, 276–293. doi: 10.1016/j.neuron.2018.09.040
- Takahashi, H., Arstikaitis, P., Prasad, T., Bartlett, T. E., Wang, Y. T., Murphy, T. H., et al. (2011). Postsynaptic TrkC and presynaptic PTP σ function as a bidirectional excitatory synaptic organizing complex. *Neuron* 69, 287–303. doi: 10.1016/j.neuron.2010.12.024

- Takahashi, H., and Craig, A. M. (2013). Protein tyrosine phosphatases PTP δ , PTP σ , and LAR: presynaptic hubs for synapse organization. *Trends Neurosci.* 36, 522–534. doi: 10.1016/j.tins.2013.06.002
- Takahashi, H., Katayama, K., Sohya, K., Miyamoto, H., Prasad, T., Matsumoto, Y., et al. (2012). Selective control of inhibitory synapse development by Slitrk3-PTP δ trans-synaptic interaction. *Nat. Neurosci.* 15, 389–398. doi: 10.1038/nn.3040
- Tarassov, K., Messier, V., Landry, C. R., Radinovic, S., Serna Molina, M. M., Shames, I., et al. (2008). An *in vivo* map of the yeast protein interactome. *Science* 320, 1465–1470. doi: 10.1126/science.1153878
- Terry-Lorenzo, R. T., Torres, V. I., Wagh, D., Galaz, J., Swanson, S. K., Florens, L., et al. (2016). Trio, a rho family GEF, interacts with the presynaptic active zone proteins piccolo and bassoon. *PLoS One* 11:e0167535. doi: 10.1371/journal.pone.0167535
- Thompson, K. M., Uetani, N., Manitt, C., Elchebly, M., Tremblay, M. L., and Kennedy, T. E. (2003). Receptor protein tyrosine phosphatase sigma inhibits axonal regeneration and the rate of axon extension. *Mol. Cell. Neurosci.* 23, 681–692. doi: 10.1016/s1044-7431(03)00120-9
- Um, J. W., Kim, K. H., Park, B. S., Choi, Y., Kim, D., Kim, C. Y., et al. (2014). Structural basis for LAR-RPTP/Slitrk complex-mediated synaptic adhesion. *Nat. Commun.* 5:5423. doi: 10.1038/ncomms6423
- Wei, Z., Zheng, S., Spangler, S. A., Yu, C., Hoogenraad, C. C., and Zhang, M. (2011). Liprin-mediated large signaling complex organization revealed by the liprin- α /CASK and liprin- α /liprin- β complex structures. *Mol. Cell* 43, 586–598. doi: 10.1016/j.molcel.2011.07.021
- Weng, Y.-L., Liu, N., DiAntonio, A., and Broihier, H. T. (2011). The cytoplasmic adaptor protein Caskin mediates Lar signal transduction during *Drosophila* motor axon guidance. *J. Neurosci.* 31, 4421–4433. doi: 10.1523/JNEUROSCI.5230-10.2011
- Wentzel, C., Sommer, J. E., Nair, R., Stiefvater, A., Sibarita, J. B., and Scheiffele, P. (2013). mSYD1A, a mammalian synapse-defective-1 protein, regulates synaptogenic signaling and vesicle docking. *Neuron* 78, 1012–1023. doi: 10.1016/j.neuron.2013.05.010
- Wong, M. Y., Liu, C., Wang, S. S. H., Roquas, A. C. F., Fowler, S. C., and Kaeser, P. S. (2018). Liprin- α 3 controls vesicle docking and exocytosis at the active zone of hippocampal synapses. *Proc. Natl. Acad. Sci. U S A* 115, 2234–2239. doi: 10.1073/pnas.1719012115
- Woo, J., Kwon, S.-K., Choi, S., Kim, S., Lee, J.-R., Dunah, A. W., et al. (2009). Trans-synaptic adhesion between NGL-3 and LAR regulates the formation of excitatory synapses. *Nat. Neurosci.* 12, 428–437. doi: 10.1038/nn.2279
- Yoshida, T., Shiroshima, T., Lee, S.-J., Yasumura, M., Uemura, T., Chen, X., et al. (2012). Interleukin-1 receptor accessory protein organizes neuronal synaptogenesis as a cell adhesion molecule. *J. Neurosci.* 32, 2588–2600. doi: 10.1523/JNEUROSCI.4637-11.2012
- Yoshida, T., Yasumura, M., Uemura, T., Lee, S.-J., Ra, M., Taguchi, R., et al. (2011). IL-1 receptor accessory protein-like 1 associated with mental retardation and autism mediates synapse formation by trans-synaptic interaction with protein tyrosine phosphatase δ . *J. Neurosci.* 31, 13485–13499. doi: 10.1523/JNEUROSCI.2136-11.2011
- Zhang, P., Lu, H., Peixoto, R. T., Pines, M. K., Ge, Y., Oku, S., et al. (2018). Heparan sulfate organizes neuronal synapses through neuroligin partnerships. *Cell* 174, 1450.e23–1464.e23. doi: 10.1016/j.cell.2018.07.002
- Zhen, M., and Jin, Y. (1999). The liprin protein SYD-2 regulates the differentiation of presynaptic termini in *C. elegans*. *Nature* 401, 371–375. doi: 10.1038/43886
- Zürner, M., Mittelstaedt, T., tom Dieck, S., Becker, A., and Schoch, S. (2011). Analyses of the spatiotemporal expression and subcellular localization of liprin- α proteins. *J. Comp. Neurol.* 519, 3019–3039. doi: 10.1002/cne.22664
- Zürner, M., and Schoch, S. (2009). The mouse and human Liprin- α family of scaffolding proteins: genomic organization, expression profiling and regulation by alternative splicing. *Genomics* 93, 243–253. doi: 10.1016/j.ygeno.2008.10.007

Conflict of Interest Statement: The authors declare that the research was conducted in the absence of any commercial or financial relationships that could be construed as a potential conflict of interest.

Copyright © 2019 Bomkamp, Padmanabhan, Karimi, Ge, Chao, Loewen, Siddiqui and Craig. This is an open-access article distributed under the terms of the Creative Commons Attribution License (CC BY). The use, distribution or reproduction in other forums is permitted, provided the original author(s) and the copyright owner(s) are credited and that the original publication in this journal is cited, in accordance with accepted academic practice. No use, distribution or reproduction is permitted which does not comply with these terms.